Electronic excitations in finite and infinite polyenes

Paul Tavan and Klaus Schulten*
Physik-Department, Technische Universität München, James-Franck-Strasse, D-8046 Garching bei München, Federal Republic of Germany
(Received 17 December 1986)

We study electronic excitations in long polyenes, i.e., in one-dimensional strongly correlated electron systems which are neither infinite nor small. The excitations are described within Hubbard and Pariser-Parr-Pople (PPP) models by means of a multiple-reference double-excitation expansion [P. Tavan and K. Schulten, J. Chem. Phys. **85**, 6602 (1986)]. We find that quantized "transition" momenta can be assigned to electronic excitations in finite chains. These momenta link excitation energies of finite chains to dispersion relations of infinite chains, i.e., they bridge the gap between finite and infinite systems. A key result is the following: Excitation energies E in polyenes with N carbon atoms are described very accurately by the formula $E^{\beta}=\Delta E_0^{\beta}+\alpha^{\beta}k(N)q$, $q=1,2,\ldots$, where β denotes the excitation class, ΔE_0^{β} the energy gap in the infinite system $[\alpha^{\beta}k(N)>0]$, and $k(N)$ the elementary transition momentum. The parameters ΔE_0^{β} and α^{β} are determined for covalent and ionic excitations in alternating and nonalternating polyenes. The covalent excitations are combinations of triplet excitations T, i.e., T, TT, TTT, ... The lowest singlet excitations in the infinite polyene, e.g., in polyacetylene or polydiacetylene, are TT states. Available evidence proves that these states can dissociate into separate triplets. The bond structure of TT states is that of a neutral soliton-antisoliton pair. The level density of TT states in long polyenes is high enough to allow dissociation into separate solitons.

I. INTRODUCTION

Motivated by the aim to develop conducting and semiconducting organic materials the properties of conjugated polymers, in particular, the properties of their prototype *trans*-polyacetylene [*trans*-$(CH)_x$] (see Fig. 1), have been investigated in recent years.[1] The investigations have been guided by solid-state-physics concepts developed for "infinite"-size materials, i.e., materials characterized by bands of very densely spaced electronic states. However, the organic conductors and semiconductors investigated so far are by no means infinite. Polyacetylene, for instance, consists of strands of conjugated polymers, called polyenes, which are some hundred carbon atoms long. It is not known how densely spaced the electronic excitations in such chains actually are and to what extent a mixing of electronic states is possible. In this paper we will attempt to bridge the gap between finite and infinite polyenes. The results will be rewarding: an extrapolation of the well-known properties of small polyenes[2] to very long polyenes provides an estimate of the density of states of finite, but long polyenes, yields explanations for previous observations, suggests new observations, and sheds light on the concepts employed so far to understand the properties of semiconducting organic polymers.

The concept that has been envoked most often in the field of organic polymers in the recent past is that of the soliton, i.e., of a low-energy excitation that involves a strong coupling between electronic and lattice degrees of freedom. It has been suggested that solitonic excitations mediate the conductivity of $(CH)_x$. In the pioneering work of Su, Schrieffer and Heeger the electron-phonon coupling had been emphasized at the expense of electron-electron interactions which had been neglected.[3,4] Subsequent theoretical studies on conjugated polymers have attempted, therefore, to evaluate the effect of electron-electron interactions on the energies and lattice structures of solitonic excitations in electron-phonon models of polyacetylene.[5-11]

Solitonic excitations as suggested by Su, Schrieffer, and Heeger have not been observed in small polyenes. What has been observed are vibronic effects on isolated electronic states, e.g., shifts of equilibrium geometries and vibrational frequencies upon excitations from the ground state to isolated excited states. The question arises whether the properties of long polyacetylene strands $(CH)_x$ arise from isolated stationary, delocalized states as in shorter polyenes or whether wave packets combined from nearly degenerate delocalized electronic excitations and shaped by a coupling to lattice distortions manifest themselves. Solitons belong to the latter class of excitations. For an answer to the question raised one needs to extrapolate the properties of finite polyenes to the long polyene limit in order (1) to see how the isolated electronic excitations in

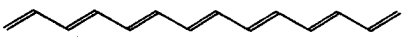

FIG. 1. Ground state of polyenes and polyacetylene characterized by alternating single and double bonds.

the short polyenes merge to form bands of excitations in the longer polyenes, (2) to obtain information on the properties of the respective excitations, e.g., their bond pattern, and (3) to estimate the intraband state density of long, but finite polyenes. This latter information determines to what extent weak interactions like electron-phonon coupling can induce new states, e.g., solitonic excitations in $(CH)_x$.

The following results of work on *finite* polyenes appear to be relevant for current investigations on polyacetylene.

(1) Qualitatively correct and quantitatively accurate descriptions of electronic spectra require highly sophisticated many-electron methods because the motion of electrons in these one-dimensional materials is dominated by Coulomb repulsion.

(2) The size of the energy gap between the ground state and the first optically allowed excited singlet state is determined by the strength of the Coulomb interaction between the π electrons; bond alternation, i.e., the pattern of single (long) and double (short) bonds, contributes only a minor fraction to the energy gap.[12,13] The first optically allowed singlet state is the lowest energy member of a class of *ionic* singlet states in polyenes which are either optically allowed or assume rather strong oscillator strengths upon a breaking of the molecular symmetry, e.g., upon trans→cis isomerization.[2]

(3) In polyenes there exist optically forbidden *covalent* singlet electronic excitations with energies below the "optical" gap. These states are characterized by collective excitations of the spin degrees of freedom of the π electrons and, therefore, do not emerge in single-electron theories as these theories largely neglect the effect of electron correlation.[14,15] The excitation energy of the covalent states depends sensitively on the degree of bond alternation, i.e., calculations of the energies of these collective π-electron excitations have to be based on realistic molecular geometries in order to render quantitative descriptions.[13] The optically forbidden character of the covalent states is not affected very much by a breaking of the molecular symmetry.

(4) The Born-Oppenheimer approximation applies to calculations of electronic wave functions. Even if pure π-electron Hamiltonians are employed for the description of polyenes the equilibrium molecular geometries in low-energy states can be estimated from calculated wave functions. These wave functions, on the other hand, are rather insensitive to the model geometry chosen for the carbon lattice, i.e., in both ground and excited states the electronic structure determines that of the lattice whereas the reverse influence is smaller. For instance, the well-known ground-state structure of alternating single and double bonds shown in Fig. 1, is revealed by bond orders that result from a calculation which assumes *equal* lengths for all polyene bonds (see also Sec. VI of this paper). Furthermore, it has been shown that excited state bond orders explain the known photochemical behavior of polyenes.[16] Hence, for a description of *finite* polyenes an inclusion of electron-phonon interaction represents an unnecessary complication.

We note that the *ionic states* are often termed *"charge-transfer" excitations* and that the *covalent states* are often referred to as *"spin-wave" excitations.*

Unfortunately, the knowledge on finite polyenes had been limited until recently[13] to short compounds with up to 10 carbons.[12,15] These compounds are too short to identify the asymptotic laws which allow an extrapolation to very long polyenes. The results obtained in Ref. 13 and in this paper alter this situation. We have presented in Ref. 13 accurate descriptions of electronic excitations for polyenes up to 16 carbons long and, in part by using results presented already there, we will reveal in this paper the asymptotic relationships that link short and very long polyenes.

The main result of previous studies on finite polyenes is that electron correlation contributes in an essential way to the properties of these compounds. Recently, the important role of electron correlation has also been deduced by observations on polyacetylene $(CH)_x$ and related materials. The occurrence of negative spin densities on alternate carbon atoms which arises due to electron-electron interaction[14] has been observed.[17] Single electron theories, in contrast to more complete theories, predict an absorption due to the neutral soliton at the "midgap" position, i.e., at a position where it has not been found.[18] Furthermore, the dependence of photocarriers on the photon energy indicates electron-hole interactions which are also not accounted for by single electron theories.[19] Consequently, the important effect of electron correlation on the physical properties of $(CH)_x$ has been emphasized.[20]

Up to now most theoretical investigations of correlation effects in $(CH)_x$ dealt with bond alternation,[21–28] with the optical gap,[12,29–31] and with solitonic excitations[5–11] in $(CH)_x$. These studies have demonstrated that an assessment of correlation effects on these properties of $(CH)_x$ depends on the quality of the approximation employed. Hartree-Fock[21,22,8] and perturbative treatments[5,23] have been shown to render qualitatively wrong predictions on the implications of electron correlations for soliton energetics[20,11] and bond alternation.[24–28] Therefore, we expect that limited configuration interaction (CI) descriptions like those in Ref. 9 strongly underestimate the effect of Coulomb interactions on soliton energetics. Any satisfactory description of electron correlation effects requires either exact solutions or extend "size-consistent" CI descriptions. Unfortunately, the enormous dimension of the many-electron Hamiltonian for polyenes with 12 and more carbon atoms makes such calculations a computationally extremely difficult task.[12] To surmount this task we have developed a new multiple-reference double-excitation configuration-interaction method (MRD-CI) which allows very accurate calculations of the low-energy spectra of polyenes comprising up to 16 carbon atoms. A detailed account of this method, a discussion of its accuracy, the results of Pariser-Parr-Pople (PPP) MRD-CI calculations on polyene spectra as well as a discussion of corresponding spectroscopic observations have been presented elsewhere.[13,32]

For an extrapolation of the properties of small ($N \leq 16$, N = number of carbon atoms) polyenes to long polyenes we investigate first the Hubbard model that is the most simple model to describe electron correlation effects in polyenes. For this model exact dispersion relations for the

infinite polyene are known.[33–37] Also for this model some of the optically allowed (ionic) excitations for *finite ring* polyenes are known exactly.[25] Accurate excitations energies for covalent states can be calculated by the MRD-CI method.[13] We demonstrate first how dispersion relations of infinite polyenes allow to approximately express electronic excitations of finite ring polyenes. This implies that we determine the momenta $k(N)$ connected with multielectron excitations in ring compounds of size N. We find that these momenta obey simple quantization rules which can be employed to express whole classes of finite polyene electronic excitations by means of infinite polyene dispersion relations.

We then attempt to link infinite Hubbard chain dispersion relations to excitation energies in *finite* open Hubbard *chains* of size N. The latter excitation energies are determined by our numerical procedure. We discover, in fact, a simple asymptotic ($N\rightarrow\infty$) behavior for finite Hubbard chains and, thereby, demonstrate that electronic excitations of finite compounds can be extrapolated accurately to the infinite compound. Next, we follow the same procedure to link finite and infinite polyenes as described by the so-called PPP model. This model provides a realistic description of the long-range character of the electron-electron interaction. Fortunately, the results show a close similarity between the asymptotic ($N\rightarrow\infty$) behavior of Hubbard and PPP chains. This finding justifies extrapolation of finite polyene calculations to polyacetylene and polydiacetylene. The following properties are investigated: (1) the structure of the bands of ionic and of covalent electronic excitations, (2) the level density of these bands as a function of chain length, (3) the bond structure of ground state and ionic and covalent excited states.

An important result of our paper is the characterization of a band of covalent states in infinite polyenes with a band edge below that of the conduction band. The expectation[15] that a band of "homopolar,"[34] i.e., covalent, excited states should exist in this energy region has been expressed already previously. This expectation originates from observations on smaller polyenes. As mentioned above it had been demonstrated, that the optically allowed polyene ^1B_u state, which gives rise to the conduction band of $(CH)_x$,[12] is not the lowest excited singlet state in these molecules. Contrary to the predictions of single-electron theories a strongly correlated "covalent" ^1A_g state[38] was found to be the lowest singlet excitation and, consequently, to be involved in the photophysics and photochemistry of polyenes.[2] Spectroscopic observations and a theoretical description revealed that the energy gap between the excited ^1B_u and the excited ^1A_g state increases with increasing polyene length,[15] a result which suggests the expectation of a low-lying covalent band in $(CH)_x$. The ^1A_g state has been inferred also to explain the long-lived 1.2 eV luminescence observed at low temperatures in $(CH)_x$.[39,40] It is the aim of this paper to substantiate the previous speculations on the band of covalent states and to discuss its relation to so-called midgap excitations.

Our paper is structured as follows. In Sec. II we introduce the MRD-CI method, the Hubbard, and PPP model Hamiltonians and describe briefly the interaction parameters assumed in our calculations. In Sec. III we review the characterization of the classes of electronic excitations in small polyenes. In Sec. IV we investigate the asymptotic behavior of excitations in Hubbard rings and Hubbard chains. In this section we provide the conceptual basis of our subsequent discussions. In Sec. V we extend the investigation to polyenes described by the PPP model. This section and the following sections deal with the properties of realistic molecular systems. In Sec. VI we discuss the bond structure of excitations in very long polyenes as described by the PPP model. In Sec. VII we provide explanations of previous observations on polyacetylene and polydiacetylene compounds and add suggestions for new observations which might reveal the character of mid-gap excitations in polyacetylene. Section VIII summarizes the results and states open questions.

II. METHODS

In this section we will briefly introduce Hamiltonians and computational methods employed in our calculations. The Hamiltonians were chosen to represent the π electrons in the polyenes and polyacetylene, and in particular, the effect of electron correlation. For this purpose the π-electron Hamiltonians must include at least a kinetic energy term that describes the delocalization of electrons, and a Coulomb repulsion term that induces electron correlation. The most simple Hamiltonian of this kind is the Hubbard Hamiltonian

$$H_{\text{Hub}}=t\sum_{\substack{n,m,\sigma\\ n\neq m}}{}' c_{n\sigma}^{\dagger}c_{m\sigma}+U\sum_{n,\sigma}c_{n,\sigma}^{\dagger}c_{n,\sigma}c_{n,-\sigma}^{\dagger}c_{n,-\sigma} \tag{1}$$

which characterizes electron systems by a single parameter $U/|t|$. The fermion creation (annihilation) operators $c_{n\sigma}^{\dagger}$ ($c_{n\sigma}$) in this Hamiltonian position the π electrons in an orthornormal set of atomic orbitals labeled by n,m. The first term in (1) represents the kinetic energy where the corresponding sum includes only nearest-neighbor sites $n=m\pm1$. The second term describes the repulsion between π electrons, the latter interaction being restricted to situations when two π electrons reside at the same atomic site n. The Hubbard Hamiltonian had been considered for polyenes also in Ref. 2 and by Soos and Ramasesha.[12]

The effective Hamiltonian most often employed for the description of electronic excitations in polyenes is that originally suggested by Pariser, Parr, and Pople (PPP).[41] This Hamiltonian assumes that the motion of σ and π electrons is separable and accounts only for the π electrons. We have employed the PPP Hamiltonian previously to describe the spectra of polyenes with up to 10 carbons.[2,14,15,38] The results were in good agreement with spectral observations on these polyenes. We have chosen, therefore, the PPP Hamiltonian also for our work presented in this and a preceding paper[13] which extend our previous descriptions to long polyenes and polyacetylene. The PPP Hamiltonian employed is in second quantization

$$H_{\mathrm{PPP}}=\sum_{n<m}U_{nm}+\sum_{m,\sigma}\left[-I-\sum_{n\neq m}U_{nm}\right]c^{\dagger}_{m\sigma}c_{m\sigma}+\sum_{\substack{n,m,\sigma\\ n\neq m}}{}'\,t_{nm}c^{\dagger}_{n\sigma}c_{m\sigma}+\frac{1}{2}\sum_{\substack{n,m,\sigma,\rho\\ (n,\sigma)\neq(m,\rho)}}U_{nm}c^{\dagger}_{n\sigma}c_{n\sigma}c^{\dagger}_{m\rho}c_{m\rho}\ . \tag{2}$$

The first term describes nuclear repulsion, the second term attraction between π electrons and nuclear cores, the third term the kinetic energy of the π electrons, and the last term their mutual Coulomb repulsion. The latter is not restricted to an intra-atomic interaction as in Eq. (1) but extends over the whole molecule. The effective Coulomb repulsion integrals between π electrons at sites n and m are given by the Ohno formula[42]

$$U_{nm}=\frac{U}{(1+0.6117r_{nm}^{2})^{1/2}}\ . \tag{3}$$

With a choice of 11.26 eV for the repulsion energy U of two π electrons at the same atomic site the two-electron matrix elements U_{nm} asymptotically, i.e., at long distances r_{nm}, approach the Coulomb interaction $U(r_{nm})=e^2/r_{nm}$, whereas at short distances the interelectronic forces correspond to those described by the Hubbard model with $U/|t|=1.53$.

In order to study the effect of a possible screening of the π-electron Coulomb repulsion due to the presence of electrons in the σ core[6-8] we have assumed in some of our calculations a short-range Coulomb interaction

$$U^{\mathrm{sc}}(r)=U(2r)\ , \tag{4}$$

which we actually described by scaling the distances r_{nm} in (3) by a factor of 2. At large distances this choice implies a dielectric screening like that in a medium with an optical density $n^2=2$. At short distances the choice entails increased interelectronic forces corresponding to those described by the $U/|t|=1.95$ Hubbard model.

Polyenes and polyacetylene assume a bond structure that features an alternation of double (short) and single (long) bonds. This bond alternation will be described in our calculations by a parameter δ which measures the difference of the lengths of single and double bonds. We will consider two models for the polyene geometry, that corresponding to an intermediate degree of bond alternation as observed in rather short polyenes ($N\approx 10$) and as described by $\delta=0.10$ Å, and that corresponding to equal bond lengths as described by $\delta=0$. The bond length affects the resonance integral t in the PPP Hamiltonian (2) that connects neighboring sites. The resonance integral can be expressed in terms of δ and is given by (distances δ in Å)

$$t=-2.4(1.0\pm 0.7\delta)\ \mathrm{eV}\ , \tag{5}$$

where the + and − signs refer to double and single bonds, respectively. In our calculations employing the Hubbard model we have considered only polyenes without bond alternation, i.e., with $\delta=0$.

The parameterization of the PPP Hamiltonian characterized above is identical to that employed by Soos *et al.* in their exact valence bond calculations on small ($N\leq 12$) polyenes.[12,43,44] The interaction parameters deviate slightly from those in our previous work[2,14,15,38] and have been adopted to allow comparisons with the results of these authors.[13]

Approximate values for the bond lengths l_n, $n=1,\ldots,N-1$ between neighboring sites n and $n+1$ can be predicted because of the π-bond orders p_n. The bond orders, defined separately for each electronic state, are the off-diagonal elements $S_{n,n+1}$ of the one-electron density matrix in the atomic orbital basis. The bond lengths can be evaluated by means of the empirical formula (bond lengths l_n in Å)

$$l_n=1.5274-0.2105p_n\ . \tag{6}$$

Equation (6) represents the linear interpolation which reproduces the observed single- and double-bond lengths for polyenes with four (butadiene) and six carbons.[45,46] The bond orders to be used for this purpose are those from a PPP-MRD-CI[13] calculation for a zeroth order polyene geometry described by $\delta=0.10$ Å.

To simplify the discussion in Sec. VI on polyene geometries in different electronic states we will use the order parameter Δl_n defined by

$$\Delta l_n=(-1)^n(l_n-\bar{l})\ , \tag{7}$$

where $\bar{l}$ is the average bond length in the respective state. The order parameter measures the degree of bond alternation in a polyene and allows a simple identification of solitonic excitations.

In order to describe accurately the spectra of the Hamiltonians in Eqs. (1) and (2) as well as the electronic properties of the corresponding electronic states we have applied the multiple-reference double-excitation configuration–interaction (MRD-CI) method presented in some detail in Refs. 13 and 32. The MRD-CI scheme[47] is characterized by an individual selection of the CI basis for each electronic state. First, the so-called "reference configurations" are determined that describe the main contributions to the respective wave function and define the unperturbed state. Then all those configurations are included into the CI expansion that in second-order perturbation theory can give an energy correction to the unperturbed state. The dimension of the resulting MRD-CI eigenvalue problem depends on the choice of the unperturbed state, on the size of the electron system as well as on the physical nature of the respective state. The MRD-CI basis may comprise up to several 10^4 spin-adapted, antisymmetrized functions. For all polyene states investigated in this paper the description of the unperturbed states has been chosen identical to that presented in Ref. 13. An exception is the ground state of the PPP model without bond alternation ($\delta=0$). For this state we have chosen only two reference configurations instead of three as in Ref. 13, resulting in a reduction of the predicted excitation energies by ≈ 0.2 eV. With this choice we achieved a uniform and consistent description of all polyene states in all models considered here. Among these models only the MRD-CI description of the extremely

strong correlation effects in the $U/|t|=4$ Hubbard model deserves additional consideration.[48] But for the remaining cases all MRD-CI calculations of polyene ground states are based on a two reference description, for all ionic excited states one reference has been employed and for all covalent excited states the description has been chosen identical to that of the first excited state presented in Ref. 13.

III. CLASSIFICATION OF POLYENE EXCITED STATES

In the following discussions we will refer to electronic states of polyenes by the symbols A_g and B_u employing the notation of the C_{2h}-symmetry point group.[2] The polyene states are eigenstates of the total spin operator. A singlet total spin is indicated by the superscript 1 in the symbols ^1A_g and ^1B_u. To denote a triplet state the superscript 1 is replaced by 3. We will consider mainly singlet states because ground state and electronic states reached first after optical excitation and internal conversion are of the singlet variety.

The PPP and Hubbard Hamiltonians give rise to yet another symmetry, the so-called "Pariser alternancy symmetry" or "particle-hole symmetry" (see Refs. 49 and 50). This symmetry classifies $-$ states, e.g., the ground state as $^1A_g^-$, and $+$ states, e.g., the lowest optically allowed state as $^1B_u^+$. Though only approximate for real molecules the alternancy symmetry is useful for two reasons. First, it allows to reduce the computational effort by taking advantage of the fact that the PPP and Hubbard many-electron Hamiltonians do not mix $^1A_g^-$, $^1A_g^+$, $^1B_u^-$, and $^1B_u^+$ states. Of course, we have taken advantage of this chance. Second, the alternancy symmetry provides a very simple classification of *ionic* states which are $+$, and *covalent* states which are $-$. We will, therefore, refer to *ionic states of polyenes and polyacetylene by an index* $+$, and to *covalent* states by an index $-$.

The classification of the electronic states is complete when one numbers the states of each symmetry class as 1,2,... in the order of increasing energy. In this notation the ground state is referred to as $1\,^1A_g^-$.

Below we will also consider electronic excitations of Hubbard ring molecules with $N=4n+2$, $n=1,2,\ldots$, carbon atoms. The excitations can be classified according to the D_{Nh}-symmetry point group. The classes of excitations which we will consider derive from the point group D_{6h}. The symmetry labels for the many-electron states which involve only π electrons are A_g, B_{1u}, B_{2u}, E_{1u}, E_{2g}. For the definition of these classes see Ref. 51. Pariser's alternancy symmetry applies within the Hubbard model to the ring compounds as well and, hence, the excitations can be further labeled as $+$ and $-$ states. For the singlet states the classifications of Hubbard ring excitations are then $1\,^1B_{1u}^-$, $1\,^1E_{2g}^+$, etc.

IV. HUBBARD RINGS AND CHAINS

Before we investigate the PPP model that provides a rather realistic description of polyenes we consider the less realistic Hubbard model since for this model exact results for the infinite system as well as for finite systems are available. Comparisons of our MRD-CI results on the low-lying singlet excitations of finite systems with exact results on finite as well as on infinite systems will serve us to test how our MRD-CI results on finite systems can be extrapolated to the infinite polyene limit, i.e., to polyacetylene $(CH)_x$. Our analysis of the size dependence of the low-lying excitations of Hubbard rings and Hubbard chains in this section will reveal features that are remarkably similar to those presented in Sec. V for the PPP model.

A. Dispersion relations of the infinite Hubbard chains and their relationship to electronic excitations in finite chains

The electronic excitations of the infinite Hubbard chain form bands which can be classified by certain quantum numbers which derive from the well-known Bethe ansatz.[52] A most recent study of the subject is that by Woynarovich[35-37] which provided analytical expressions for the dispersion relations of the bands of electronic excitations in the infinite Hubbard chain. In the following we will consider three dispersion relations which we determined according to the expressions provided by Woynarovich: (1) the dispersion relation for the band of ionic singlet states denoted by $E^+(k)$, where k is the momentum variable; (2) that for the lower edge of the band of covalent singlet excitations denoted by $E^{1-}(k)$; (3) that for the covalent singlet excitations characterized by four holes in the λ distribution[37] denoted by $E^{4-}(k)=\sum_{s=1}^{4}E^{1-}(k_s)$ with $k=\sum_{s=1}^{4}k_s$. This latter dispersion relation describes the upper edge of the band of covalent singlet states. All dispersion relations depend, of course, parametrically on the Hubbard parameter $U/|t|$.

The lowest transitions to ionic and covalent states of the infinite Hubbard chain have vanishing momenta k. The corresponding excitation energies—the "optical gap" $E^+(0)$ and the "covalent gap" $E^-(0)$—have values $E^+(0)\neq 0$ and $E^{1-}(0)=E^{4-}(0)=0$, respectively. The question arises if the *infinite* chain dispersion relations can also provide an approximate description of the lowest excitation energies for *finite* Hubbard chains. For an answer to this question one has to consider that finite molecules cannot accommodate electronic states with vanishing momenta and that finite size molecules do not conserve momentum upon electronic excitation.

An estimate for the smallest momentum change k involved in an electronic excitation of a finite polyene can be obtained by considering the $U=0$ case for which analytical expressions for the excitation energies exist. In this case the analytical descriptions of the excitation energies $E(N)$ in finite rings and chains derive from the dispersion relations $E(k)$ of the infinite chain. A straightforward calculation yields the following dispersion relation $E(k)$ for the energetically lowest particle-hole excitation

$$E(k)=4|t|\sin(k/2)\,, \tag{8}$$

where k is the momentum change connected with the excitation and where the lattice constant has been chosen to be unity. In finite systems the minimum values of k are

$$k^r(N)=\frac{2\pi}{N} \tag{9}$$

for *rings* with $N=4n+2$ carbon atoms, and

$$k^c(N)=\frac{\pi}{N+1} \tag{10}$$

for *chains* with $N=2n$ carbon atoms. The analytical expressions for the excitation energies $E_1^r(N)$ and $E_1^c(N)$ of the lowest particle-hole excitations in rings and chains, respectively, are now obtained by inserting k^r and k^c given by Eqs. (9) and (10) into the dispersion relation given by Eq. (8). Similarly, excitation energies E_q^r and E_q^c for further transitions are obtained if one inserts multiples of k^r and k^c into Eq. (8), i.e., for the rings the momenta

$$k_q^r=qk^r \tag{11}$$

and for the chains the momenta

$$k_q^c=qk^c\ , \tag{12}$$

where $q=1,2,\ldots$ defines a *momentum quantum number* characteristic for the respective transition. From now on we will use the term *transition momentum* for the momentum change involved in an electronic excitation.

For a system of independent electrons the transition momenta are solely determined by the geometry of the molecule. In a correlated electron system the character of an excitation can depend on the strength of the electron-electron repulsion U. For such excitations the transition momenta can vary with U. If the character of the excitation is independent of U, the values of the transition momenta provided by Eqs. (8)–(12) for the $U=0$ case apply to all U values. This is the case, actually, for finite Hubbard rings for which the total momenta[37] of the charge-transfer as well as of spin-wave excitations are integer (or half-odd integer) multiples of k^r such that the transition momenta are integer multiples of k^r as expressed by Eq. (11).[37] However, in the finite open Hubbard chains, for which no general statements on the functional form of the transition momenta can be made (see below), the character of the excitations can depend on U. We suggest, therefore, that the transition momenta are given by

$$k_q^{c\beta}(N,U)=q\gamma_q^\beta(U)k^c(N) \tag{13}$$

with k^c defined by Eq. (10), $\beta\in\{+,1-,4-\}$, $q=1,2,\ldots$, and $\gamma_q^\beta(U)\geq 1$. Values $\gamma_q^\beta(U)>1$ can be interpreted as an effective shortening of the chains due to electron correlation.

Up to now the transition momentum quantum numbers q have been determined only for two low-lying ionic excitations in finite correlated Hubbard rings (see below and Ref. 53). The quantum numbers q associated with the transitions to the other ionic states and to the covalent states are still unknown because the Lieb-Wu equations[33] have not yet been solved for these cases. For the linear chains no analytical results on quantum numbers and transition momenta are available since equations that are analogous to the Lieb-Wu equations for the rings have not been derived yet. In particular, there exists no rigorous justification for the suggestion in Eq. (13) concerning the transition momenta k_q^β, such that this suggestion merely represents an attempt of a simple generalization of the $U=0$ case. But for the moment, to avoid an unnecessary complication of the following discussion, we will assume that the finite chain transition momenta are independent of U and, hence, given by Eq. (12) instead by Eq. (13). Only later, for those cases, for which the generalization (13) cannot be avoided, we will use this generalization and try to determine, thereby, the scaling factor $\gamma_q^\beta(U)$.

For $U\neq 0$ we would like to conjecture now that the dispersion relations when combined with the transition momenta provide approximate excitation energies for finite systems. Thus the excitation energies for finite Hubbard *ring* molecules are approximated by the composite functions $E_q^{r\beta}=E^\beta\circ k_q^r$ defined by

$$E_q^{r\beta}(N)=E^\beta\left[q\frac{2\pi}{N}\right] \tag{14}$$

and for open *chains* by the composite functions $E_q^{c\beta}=E^\beta\circ k_q^c$ defined by

$$E_q^{c\beta}(N)=E^\beta\left[q\frac{\pi}{N+1}\right] \tag{15}$$

with $\beta\in\{+,1-,4-\}$ and $q=1,2,\ldots$. In case that the generalization (13) should apply to the chain transition momenta, the excitation energies should be approximately given by inserting the transition momenta $k_q^{c\beta}(N,U)$ instead of the momenta $k_q^c(N)$ into the dispersion relations E^β. Independently of the choice of the functional form of the chain momenta, however, those intervals of the dispersion relations $E^\beta(k)$ that are linear in k, should give rise to a linear behavior of the excitation energies for finite rings on a $1/N$ scale and for finite chains on a $1/(N+1)$ scale. These conjectures will be investigated now.

B. Hubbard rings

The excitation energies for the *ionic* states $1\,^1E_{1u}^+$ and $1\,^1E_{2g}^+$ of finite Hubbard rings with $N=4n+2$ atoms (see Sec. III for the nomenclature) have been determined by Hashimoto[53] by an exact numerical solution of the Lieb-Wu equations.[33] The excitation energies of the $1\,^1E_{1u}^+$ state evaluated by Hashimoto for weak ($U/|t|=1.25$), medium ($U/|t|=2.08$), and strong ($U/|t|=5$) electron-electron repulsion are presented in Fig. 2 on a $1/N$ scale. It should be noted here that realistic polyenes correspond to a $U/|t|$ ratio of 1.5.

The transition momentum associated with the $1\,^1E_{1u}^+$ excitation is $2\pi/N$, i.e., the momentum quantum number has the value $q=1$.[53] In order to test our suggestion that the dispersion relation E^+ of the conduction band of the infinite Hubbard chain provides an estimate of the low-lying ionic excitations of finite ring molecules we provide also in Fig. 2 the excitation energies $E_1^{r+}(N)$ resulting from Eq. (14).

Figure 2 demonstrates that the exact excitation energies of the $1\,^1E_{1u}^+$ state for large N converge to the function E_1^{r+}. In fact, in the cases of weak and intermediate electron-electron repulsion the exact excitation energies for all ring sizes follow closely the excitation energy function E_1^{r+} derived from the dispersion relation E^+. Be-

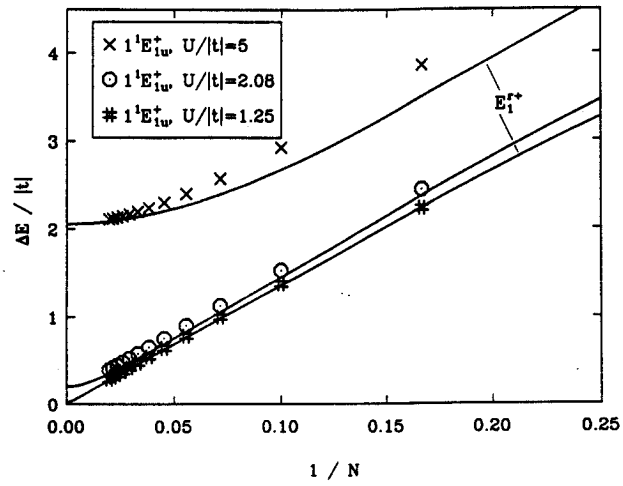

FIG. 2. Exact excitation energies of the energetically lowest ionic singlet state in the Hubbard model of *cyclic* polyenes for the cases of weak ($U/|t|=1.25$), intermediate ($U/|t|=2.08$), and strong ($U/|t|=5.0$) electron correlation. The excitation energies of the $1\,^1E_{1u}^+$ state of the $N=4n+2$, $n=1,\ldots,12$, rings are compared with the corresponding energies E_1^{r+} of the infinite system, which are defined by the momentum $k_1^r=2\pi/N$ of the $1\,^1E_{1u}^+$ state. The $1\,^1E_{1u}^+$ excitation energies have been adopted from Hashimoto's work (Ref. 53) and the dispersion relations E^+ have been calculated according to the results of Woynarovich (Ref. 35).

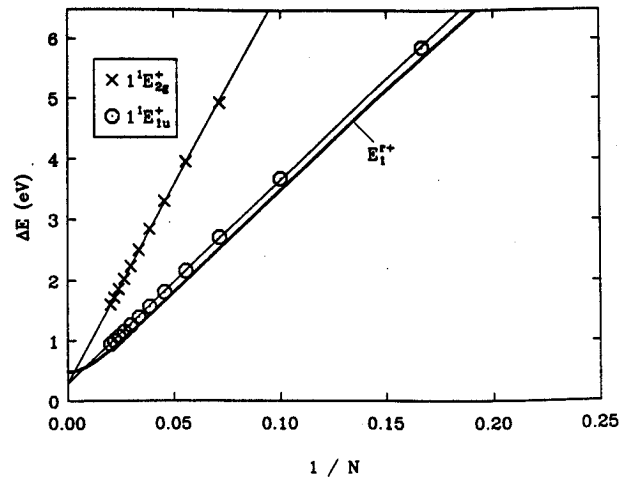

FIG. 3. Linear $1/N$ extrapolations of the exact excitation energies (Ref. 53) of the first ($1\,^1E_{1u}^+$) and a the third ($1\,^1E_{2g}^+$) ionic singlet state of finite polyene rings described by the Hubbard model for the case of intermediate electron correlation ($U/|t|=2.08$, $|t|=2.4$ eV). For comparison also the excitation energies E_1^{r+} of the infinite system (Ref. 35) are shown at the momentum $k_1^r=2\pi/N$ of the $1\,^1E_{1u}^+$ state. The $1\,^1E_{1u}^+$ states extrapolate (lower straight line) at $1/N=0$ to an optical gap $\Delta E^+=0.29$ eV, i.e., slightly below the exact value $E^+(0)=0.4789$ eV given by the zero momentum limit of the E^+ dispersion relation. The $1\,^1E_{2g}^+$ states extrapolate (upper straight line) also to 0.29 eV. The slopes of the two extrapolations differ by a factor of 1.95.

cause $E_1^{r+}\sim N^{-2}$ in the limit of large N, this agreement implies that also the excitation energies for large N converge as N^{-2} to the infinite chain optical gap. In the case of weak and intermediate electron-electron repulsion the size dependence actually behaves as N^{-1} for rings with up to 100 atoms and assumes the N^{-2} dependence only for larger rings. The latter deviation from the N^{-1} dependence for weak and intermediate electron-electron repulsion is very small. Consequently, for an estimate ΔE_0 of the optical gap in polyacetylene with a known $U/|t|$ ratio of about 1.5, one can extrapolate the excitation energies of finite rings as N^{-1}, i.e., describe the excitation energies by the simple functional dependence

$$\Delta E=\Delta E_0+\alpha/N \tag{16}$$

without introducing a large error. However, because of the asymptotic N^{-2} dependence the gap energy ΔE_0 in this equation will always underestimate the true gap energy $E^+(0)$.

The results in Fig. 2 represent only the lowest lying optically allowed $1\,^1E_{1u}^+$ state of Hubbard rings. In Fig. 3 we compare for intermediate electron-electron repulsion ($U/|t|=2.08$) the excitation energies of the $1\,^1E_{1u}^+$ state with those of the $1\,^1E_{2g}^+$ state. The $1\,^1E_{2g}^+$ state is the third ionic state in Hubbard rings and according to Hashimoto[53] is characterized by a value $q=2$ of the transition momentum quantum number. (The second ionic state, which is not shown in Fig. 3, is of $^1B_{1u}^+$ symmetry. Due to the degeneracy of the orbital pattern of the $N=4n+2$ rings this state is nearly degenerate with the $1\,^1E_{1u}^+$ state.[54] Unfortunately, no exact results on the $1\,^1B_{1u}^+$ state are available up to now). The size dependence of the exact excitation energies has been fitted for both ionic states to expressions of the type (16). The energy gaps ΔE_0 resulting for the two transitions are identical (0.29 eV) and underestimate the exact value of $E^+(0)=0.48$ eV. The slopes α for the two excitations differ by a factor of 1.95. This value is close to the value $q=2$ expected from predictions based on the dispersion relation E^+: These predictions assign the excitation energies $E_1^{r+}(N)$ to the $1\,^1E_{1u}^+$ state and $E_2^{r+}(N)$ to the $1\,^1E_{2g}^+$ state. The close to linear $1/N$ behavior of E_1^{r+} and E_2^{r+} in the range $10<N<50$ implies that the slopes α in Eq. (16) yield information on the momentum quantum numbers q to be attributed to the electronic excitations. Thus, the energies for ionic excitations of Hubbard rings actually follow the approximate law

$$\Delta E=\Delta E_0+q\alpha/N,\quad q=1,2,\ldots. \tag{17}$$

We will consider the size dependence of the excitation energies involving the *covalent* states. Figure 4 provides the excitation energies of the two lowest covalent singlet states $1\,^1B_{1u}^-$ and $1\,^1E_{2g}^-$ of finite Hubbard rings in case of an intermediate electron-electron repulsion described by a $U/|t|=2$ ratio. For comparison Fig. 4 also shows the excitation energies of the lowest ionic singlet state $1\,^1E_{1u}^+$. In lieu of an analytical description these excitation energies had to be evaluated by our MRD-CI method, for

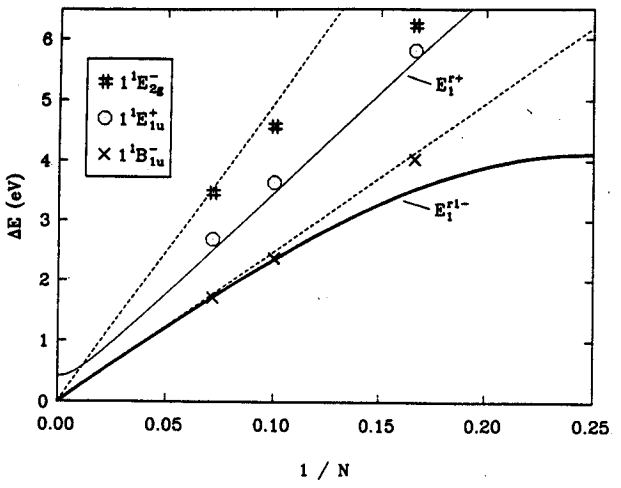

FIG. 4. For the $U/|t|=2$ Hubbard model MRD-CI excitation energies of the $1^1B_{1u}^-$ (crosses), $1^1E_{1u}^+$ (circles), and $1^1E_{2g}^-$ (double crosses) states of finite *cyclic* polyenes are compared with exact excitation energies of the infinite system at corresponding momenta. For comparison with the lowest covalent state of the rings ($1^1B_{1u}^-$) the lower edge E^{1-} of the dispersion relations of the singlet spin excitations of the infinite system (Ref. 37) has been evaluated at the momentum $k_1^r=2\pi/N$ of the $1^1B_{1u}^+$ state. The resulting excitation energies are denoted by E_1^{r1-}. Because the lowest ionic state of the rings ($1^1E_{1u}^+$) carries the same momentum the dispersion relation E^+ of the particle-hole singlet excitation have also been evaluated at this momentum. The lower dashed line is the tangent to E_1^{r1-} at $1/N=0$, the upper dashed line has twice the slope of the tangent.

which reason only data points for rings with 6, 10, and 14 atoms are available. Such limited information does not yet allow a convincing demonstration of the asymptotic behavior of covalent ring excitations. Nevertheless, the following analysis of the data shown in Fig. 4 seems to indicate that the covalent excitations follow the same pattern as the ionic excitations.

The analysis starts from a comparison of the MRD-CI excitation energies of the $1^1B_{1u}^-$ and $1^1E_{2g}^-$ states with predictions of these energies derived from the dispersion relations E^{j-}. For small k all dispersion relations $E^{j-}(k)$, $j=1,2,4$, of covalent excitations eventually become linear and the linear range extends towards larger momenta k for larger values of j.[37] Thus, all ring excitation energy functions E_q^{rj-} become linear for large N on a $1/N$ scale and the linear range extends further towards small ring sizes N for small momentum quantum numbers q and large values of j. As shown in Fig. 4 the linear range of the ring excitation energy function E_1^{r1-} ($q=1$, $j=1$) extends up to about $N=10$. The excitation energies of the lowest covalent state $1^1B_{1u}^-$ for large N approach this function from above. The tangent to the function E_1^{r1-} at $1/N\to 0$, that, according to the arguments given above, represents an even closer approximation to the function E_1^{r4-} (not shown in Fig. 4), provides an excellent approximation to the $1^1B_{1u}^-$ excitation energies for rings of all the sizes considered. Multiplication of the slope of the tangent by a factor 2, which according to Eqs. (11) and (14) yields the tangent to the function E_2^{r1-} ($q=2$), provides an asymptotic limit of the excitation energies of the second covalent state, the $1^1E_{2g}^-$ state. We expect, therefore, that the covalent excitations follow also the simple law (17) with $q=1$ for the $1^1B_{1u}^-$ state and $q=2$ for the $1^1E_{2g}^-$ state. This important observation, so far only vaguely indicated by the results in Fig. 4, will be demonstrated more convincingly for open Hubbard chains and for polyenes described by the PPP model.

The close agreement between the tangent of E_1^{r1-} at $1/N\to 0$ and the MRD-CI excitation energies of the lowest covalent state suggests that the extrapolation of the MRD-CI excitation energies on a $1/N$ scale for rings should be a reliable tool for the determination of the covalent gap $E^-(0)$. If sufficient data on large systems and on higher excited states are available such extrapolations according to (17) can also yield the covalent momentum quantum numbers q.

C. Linear Hubbard chains

We want to demonstrate now that the ionic and covalent excitations in linear Hubbard chains exhibit a size dependence of their excitation energies which is very similar to that of the ring compounds as described by Eq. (17). There exist, however, two important differences. (1) Since the chain momenta k_q^c exhibit a $1/(N+1)$ behavior instead of the $1/N$ behavior of the ring momenta, the size dependence of the chain excitation energies has to be considered on the appropriate $1/(N+1)$ scale. (2) The transition momenta k_q^{c+} of the *ionic* excitations turn out to be noninteger multiples of the elementary chain momentum k^c with a scaling factor γ depending on the degree of electron-electron repulsion.

First we want to show that Eq. (13) instead of Eq. (12) applies to the transition momenta k_q^{c+} and that the factor γ in Eq. (13) assumes values $\gamma_q^+(U)>1$ if $U/|t|>0$. For this purpose we compare in Fig. 5 the excitation energies of the lowest ($q=1$) ionic states in rings ($1^1E_{1u}^+$) and linear chains ($1^1B_u^+$) with the chain excitation energy functions E_q^{c+}, $q=1,2,$. These functions have been derived from the dispersion relations E^+ according to Eq. (15) which does not take a value $\gamma_q^+(U)\neq 1$ for $U/|t|>0$ into account.

In the case of vanishing Coulomb repulsion ($U/|t|=0$) the analytical solutions for the $1^1E_{1u}^+$ and $1^1B_u^+$ excitation energies are given by $E_1^{r+}(N)$ and $E_1^{c+}(N)$, respectively. According to Eqs. (8)–(10), (14), and (15) these functions are

$$E_1^{r+}(N)=4|t|\sin(\pi/N) \tag{18}$$

for the ring ($1^1E_{1u}^+$) states and

$$E_1^{c+}(N)=4|t|\sin[\pi/2(N+1)] \tag{19}$$

for the linear chain ($1^1B_u^+$) states. Since the ring momentum k^r, given by (9), is about two times larger than the chain momentum k^c, the ring excitation energies increase about two times faster than the chain excitation energies with decreasing molecular size N. This is exhibited in Fig. 5 by the fact, that the ring $1^1E_{1u}^+$ excitation energies

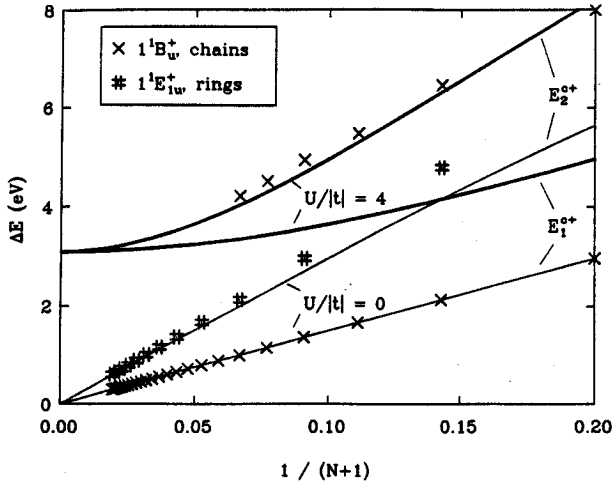

FIG. 5. The end effect on the excitation energies of the lowest *ionic* singlet state of the Hubbard model and its dependence on electron correlation. The dispersion relations E^+ for the particle-hole singlet excitation of the infinite chain evaluated at one (E_1^{c+}) and two (E_2^{c+}) quanta of the finite chain momentum $k^c=\pi/(N+1)$ [cf. Eq. (15)] are compared with the exact energies of the $1\,^1B_u^+$ state (crosses) of the finite open chains and of the $1\,^1E_{1u}^+$ state (double crosses) of the rings in the case of the uncorrelated electron system ($U/|t|=0$) and with MRD-CI excitation energies of the $1\,^1B_u^+$ state in the case of a strongly correlated electron system.

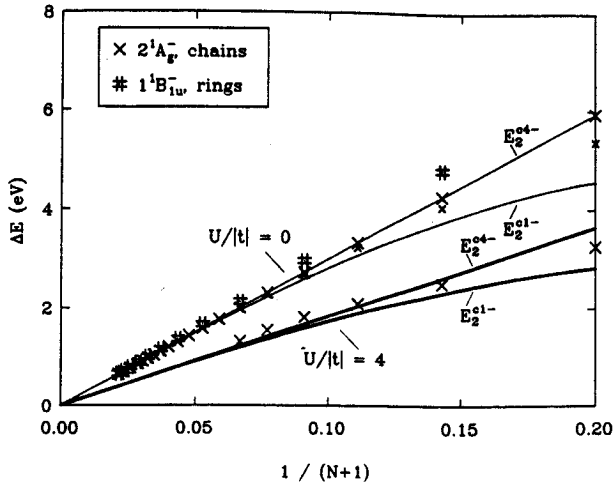

FIG. 6. The end effect on the excitation energies of the lowest *covalent* singlet state of the Hubbard model and its dependence on electron correlation. For the cases of vanishing ($U/|t|=0$) and of strong ($U/|t|=4$) electron correlation the lower edge E^{1-} of the dispersion relations of the singlet spin excitations in the infinite chain as well as the upper edge E^{4-} of these relations for excitations characterized by four holes in the λ distribution (Ref. 37) have been evaluated at two quanta of the finite chain momentum $k^c=\pi/(N+1)$ resulting in the functions E_2^{c1-} and E_2^{c4-} [cf. Eq. (15)]. In the case of strong electron correlation these functions are compared with the MRD-CI excitation energies of the $2\,^1A_g^-$ state of open chains, whereas in the case of vanishing electron correlation they are compared with the exact excitation energies of the $1\,^1B_{1u}^-$ state of the rings (double crosses) and of two $^1A_g^-$ states of the open chains. The latter states are characterized by a double excitation from the highest occupied to the lowest unoccupied molecular orbital (large crosses) and by a single excitation from the highest occupied to the second to lowest unoccupied orbital (small crosses), respectively.

($q=1$), given by Eq. (18), are located close to the excitation energies E_2^{c+} which are associated with the transition momenta $2k_c$.

The difference between the energies $E_1^{r+}(N)$ and $E_1^{c+}(N)$ has to be attributed to the "end effect." Equations (18) and (19) demonstrate that the end effect is large. This result is at variance with Hashimoto's treatment of the end effect[53] that has been based on first-order perturbation theory. This author determined that the end effect vanishes faster than $1/N$ which is obviously not true in the $U=0$ limit [cf. Eqs. (8)–(10)].

However, the end effect becomes smaller when the degree of electron-electron interaction increases. This can be concluded from a comparison in Fig. 5 of the excitation energy of the $1\,^1B_u^+$ state ($q=1$) with the excitation energy functions E_1^{c+} and E_2^{c+} for $U/|t|=4$. The former function would provide an estimate for the $1\,^1B_u^+$ excitation energies if the transition momentum k_1^{c+} would be solely determined by the geometry, i.e., given by Eq. (10). That is not the case. However the latter function which is close to the ring excitation energies $E_1^{r+}(N)$ lies also close to the $1\,^1B_u^+$ excitation energies. This implies that the chain momentum k_1^{c+} associated with the transition to the $1\,^1B_u^+$ state in the case $U/|t|=4$ is about two times larger than the momentum $k_1^{c+}=k^c$ associated with this transition in the case $U/|t|=0$. Consequently, Eq. (13) instead of Eq. (12) has to be employed for the description of the transition momenta of the ionic chain states and the factor $\gamma_1^+(U)$ increases from a value $\gamma_1^+(0)=1$ to the value $\gamma_1^+(4|t|)\approx 2$.

Figure 6 compares again for the cases $U/|t|=4$ and $U/|t|=0$ the excitation energies of the lowest *covalent* states $1\,^1B_{1u}^-$ in the ring ($q=1$) and $2\,^1A_g^-$ in the linear chain ($q=2$) with excitation energy functions derived according to Eq. (15) from the dispersion relations E^{1-} and E^{4-} assuming $q=2$. Here, the value $q=2$ for the $2\,^1A_g^-$ state derives from the fact that this state involves an excitation which promotes either a single electron across two single electron level spacings or promotes two electrons from the highest occupied to the lowest unoccupied single electron level, i.e., promotes two electrons each across a single level spacing. As one can show for the case $U=0$, the crossing of each electron level spacing adds a minimum momentum value k^c to the many electron transition.

For the case $U=0$ the ring and chain excitation energies are very close and asymptotically approach the E_2^{c1-} and the E_2^{c4-} excitation energy functions. The latter function represents the exact solution for the two-electron excitation (large crosses in Fig. 6) in linear chains. The two times larger quantum number of the lowest covalent excitation in the chains as compared to that in the rings

and the little more than two times smaller value of the elementary chain momentum k^c as compared to that of the ring momentum k^r explain why a large, $1/N$-type end effect is missing in the case of spin-wave excitations.

The excitation energies of the lowest covalent state for the $U/|t|=4$ case are seen in Fig. 6 to lie below the corresponding excitation energies for the $U/|t|=0$ case, i.e., they exhibit an ordering which is opposite to that of the ionic states for the same difference in the $U/|t|$ rations (cf. Fig. 5). This demonstrates the well-known fact that electron correlation effects decrease the excitation energies of covalent states and increase the excitation energies of ionic states. The excitation energies, which were determined by means of the MRD-CI method, asymptotically approach the E_2^{c1-} and E_2^{c4-} excitation energy functions. This behavior indicates that the momentum changes associated with the covalent states in the linear chain compounds are not affected by the degree of electron-electron repulsion, i.e., that $\gamma_q^-(U)\equiv 1$ and that Eq. (12) applies to these transition momenta.

We want to consider now in further detail the size dependence of the covalent and the ionic excitations in linear Hubbard chains. For this purpose we present in Figs. 7 and 8 the excitation energies for the case

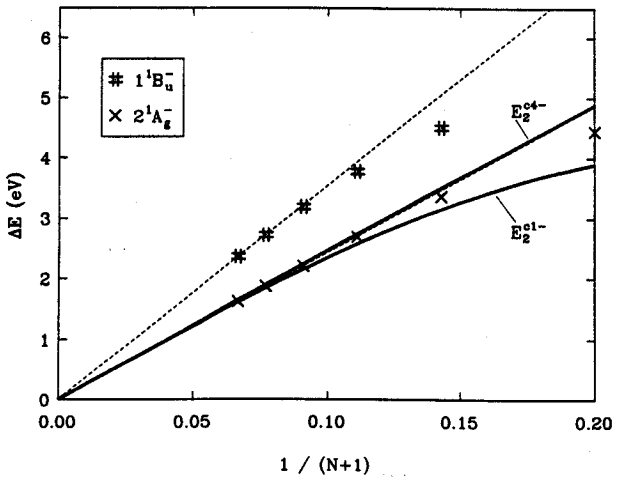

FIG. 7. Linear $1/(N+1)$ extrapolations of the Hubbard-MRD-CI excitation energies of the two lowest *covalent* singlet excitations of finite linear polyenes and comparison with corresponding excitation energies in the infinite chain for the case of intermediate electron correlation characterized by the value $U/|t|=2$ of the Hubbard parameter. The extrapolation (lower dashed line) of the $2\,^1A_g^-$ excitation energies (crosses) represents a least square deviation fit according to Eq. (20) to the MRD-CI results obtained for the $N=10$, 12, and 14 π-electron polyenes, whereas the extrapolation (upper dashed line) for the $1\,^1B_u^-$ state (double crosses) is the line connecting the excitation energies at $N=12$ and 14. The slope of the fit to the $2\,^1A_g^-$ excitation energies ($q=2$) is $\alpha=12.15$ eV and the ratio of the slopes of the two extrapolations is 1.46. For comparison with the $2\,^1A_g^-$ excitation energies the dispersion relations E^{1-} and E^{4-} of the infinite system have been evaluated at two quanta of the finite chain momentum $k^c=\pi/(N+1)$ (see text and Fig. 5 caption for further explanation).

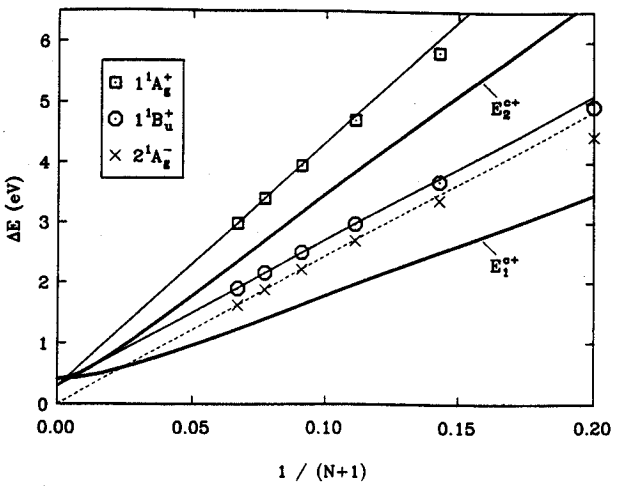

FIG. 8. Linear $1/(N+1)$ extrapolations of the Hubbard-MRD-CI excitation energies of the two lowest *ionic* singlet excitations of finite linear polyenes and comparison with corresponding excitation energies in the infinite chain for the case of intermediate electron correlation characterized by the value $U/|t|=2$ of the Hubbard parameter. As a reference the excitation energies (crosses) and extrapolation (dashed line) for the covalent $2\,^1A_g^-$ state are also shown. The extrapolation (lower solid line) of the $1\,^1B_u^+$ excitation energies (circles) represents a fit according to Eq. (20) to the MRD-CI results obtained for the $N=8$, 10, 12, and 14 π-electron polyenes, whereas the extrapolation (upper solid line) for the $1\,^1A_g^+$ state (squares) is the line connecting the excitation energies at $N=12$ and 14. The ratio of the slopes of the two extrapolations is 1.67, the extrapolated optical gap is $\Delta E^+=0.29$ eV and the slope of the fit to the $1\,^1B_u^+$ excitation energies ($q=1$) is $\alpha=24.11$ eV. For an evaluation of the end effect the $1\,^1B_u^+$ and $1\,^1A_g^+$ excitation energies are compared with corresponding excitation energies of the infinite system calculated from the dispersion relation E^+ at one (E_1^{c+}) and two (E_2^{c+}) quanta of the finite chain momentum $k^c=\pi/(N+1)$.

$U/|t|=2$ involving the two lowest covalent and ionic excitations.

Figure 7 compares the excitation energies of the two *covalent* states with the excitation energy function E_2^{c1-} derived from the dispersion relation E^{1-} according to Eq. (15) assuming $q=2$. The excitation energies of the $2\,^1A_g^-$ state approach E_2^{c1-} for large N, proving—together with the results discussed above—that the lowest lying covalent excitation carries the momentum $k_2^c=2k^c$, i.e., that Eqs. (12) and (15) in fact apply to all three strengths of electron-electron repulsion $U/|t|=0,2,4$.

In order to determine which momentum quantum number is associated with the second covalent excitation involving the $1\,^1B_u^-$ state we present in Fig. 7 the linear extrapolations connected with the two covalent excitations. The extrapolations shown vanish asymptotically as required by the fact that the covalent gap energy vanishes in the infinite Hubbard chain limit. The slopes of the two extrapolations differ by a numerical factor 1.45. This factor is close to the value $\frac{3}{2}$. Considering that $q=2$ for the

$2\,^1A_g^-$ state the latter value corresponds to a momentum quantum number $q=3$ for the $1\,^1B_u^-$ excitation. A generalization of this finding suggests that there is a class of covalent excitations in linear Hubbard chains which for large N approximately follows the law

$$\Delta E=\Delta E_0+q\alpha/(N+1) \tag{20}$$

with $q=2,3,4,\ldots$. Equation (20) is analogous to the law for rings expressed by Eq. (17). The close to linear $1/(N+1)$ behavior of the chain excitation energies will actually be documented in further detail for the PPP model in the next section.

The results in Fig. 7 on the covalent states show that one can extrapolate indeed numerical excitation energies for finite chains to the infinite chain limit by means of a $1/(N+1)$ size dependence if these extrapolations are based on excitation energies of compounds comprising 10 sites and more.

Figure 8 presents the size dependence of the excitation energies involving the two lowest lying *ionic* states. The excitation energies of the $2\,^1A_g^-$ state are also included in Fig. 8 to demonstrate for the $U/|t|=2$ linear Hubbard chain that this state lies energetically below the optically allowed ionic states.

The excitation energies of the ionic state $1\,^1B_u^+(q=1)$ are compared in Fig. 8 with the excitation energy functions E_1^{c+} and E_2^{c+} that correspond to momentum quantum numbers $q=1$ and $q=2$ according to Eq. (15). The results show that for the $U/|t|=2$ case the $1\,^1B_u^+$ excitation carries a momentum $k_1^{c+}\approx 1.5k^c$, i.e., $\gamma_1^+(2|t|)\approx 1.5$ a value which is halfway between that for the $U=0$ case and the $U=4|t|$ case.

It is of interest to determine the transition momentum k_2^{c+} associated with the second ionic excitation involving the $1\,^1A_g^+$ state. The ratio of the slopes of the linear $1/(N+1)$ extrapolations shown in Fig. 8 for the two ionic states is 1.67. If k_2^{c+} would be given according to a relation like $k_q^{c+}=qk_1^{c+}$, i.e., if the factor $\gamma_q^+(U)$ in Eq. (13) would be independent of q, one would expect a ratio of 2. There are two possible explanations for this difference. (1) The difference may be due to an accidental addition of the errors inherent to our MRD-CI description[13] and to our linear extrapolations. Thus, it may be that a ratio closer to the value 2 would result if the extrapolations were based on exact excitation energies for longer compounds. (2) The deviation of the ratio 1.67 from the value 2 indicates a true physical effect, i.e., $\gamma_q^+(U)$ decreases with increasing q. The value 1.67 implies then $\gamma_2^+(2|t|)\approx 1.25$. The U dependence of the transition momentum k_q^{c+} as well as its decrease with increasing q could be due to the development of an excitonic character of the lowest energy ionic excitations in a linear chain geometry. Such character would imply that the particle-hole binding energy decreases for decreasing electron correlation. Furthermore it could also imply that higher excitations are less affected by this excitonic binding energy, i.e., that $\gamma_q^+(U)\to 1$ for both $U\to 0$ and $q\to\infty$. Then also for the ionic transitions Eq. (12) instead of Eq. (13) should hold if higher excitations are involved and if electron correlation is small.

Figure 8 demonstrates that the linear dependence in $1/(N+1)$ is satisfied very well by MRD-CI excitation energies for the ionic states. This suggests that finite size energies can be extrapolated to the infinite chain limit for ionic states as well. However, the resulting value $\Delta E_0=0.29$ eV for the optical gap is too small compared to the exact value $E^+(0)=0.41$ eV. The error in the gap energy should be less for calculations of realistic polyenes since these systems correspond to a $U/|t|=1.5$ ratio for which the $(N+1)^{-2}$ deviation from the $1/(N+1)$ extrapolation is less significant.

V. POLYENE AND POLYACETYLENE ELECTRONIC SPECTRA IN THE PPP MODEL

We want to show in this section that close similarities exist between linear polyenes as described by the Hubbard and by the PPP Hamiltonian. The similarities are found for the asymptotic size dependence of the ionic and covalent transitions. We will further investigate in this section the effect of bond alternation on the spectra of polyenes, in particular, in the limit of the infinite polyene, i.e., polyacetylene $(CH)_x$. Lastly, we consider to what extent dielectric screening of the electron-electron repulsion influences the spectra of polyenes and polyacetylene.

In order to apply the results of Sec. IV we compare the strength of the electron-electron repulsion in the PPP and in the Hubbard model. For this purpose one has to determine the ratio $(U_{ii}-U_{ii+1})/|t|$, where U_{ij} is the Coulomb integral for electrons at sites i and j, and t is the resonance integral given by Eq. (5). Our parametrization of the PPP Hamiltonian yields the value 1.53 for this ratio. We conclude that the short-range Coulomb repulsion between the π electrons is weaker in the PPP model than in a Hubbard model with a $U/|t|=2$ ratio.

A second measure for the effect of the Coulomb repulsion in the PPP and the Hubbard model is the ground state correlation energy per site. This energy is defined as the energy difference between the SCF ground state and the ground state as described by the MRD-CI method divided by the number of carbon atoms. The ground state correlation energy per site measures about 0.15 eV for the PPP model with bond alternation, 0.18 eV for the PPP model without bond alternation,[13] and 0.25 eV for the $U/|t|=2$ Hubbard model. This comparison indicates, too, that correlation effects are weaker in the PPP model than in the $U/|t|=2$ Hubbard model. Consequently, the results on the Hubbard model let us expect that the size dependence of the spectra of the polyenes in the PPP description should obey a $1/(N+1)$ dependence as expressed by Eq. (20) for compounds with 10 carbons and more. Such dependence, actually a $1/N$ dependence, had been observed and predicted before for the optical transition to the ionic $1\,^1B_u^+$ state of polyenes.[30,55]

A. Nonalternating model polyenes

In the Hubbard model of linear polyenes as described by the Hamiltonian (1) all resonance integrals t are chosen to be identical. This implies according to Eq. (5) that all bond lengths are assumed to be equal. We will, therefore,

consider the PPP model of polyenes without bond alternation first, since that should yield the closest similarities to the results in the previous section.

Figure 9 presents our MRD-CI excitation energies for the two lowest ionic and covalent excitations in nonalternating polyenes. The calculations were carried out for polyenes with $N=4,6,\ldots,14$ carbon atoms. The results in Fig. 9 show that the excitation energies for $N=10,12,14$ follow closely a $1/(N+1)$ dependence. The gap energies and slopes resulting from a fit according to Eq. (20) to the lowest ionic ($q=1$) and covalent ($q=2$) transitions are provided in Table I. In agreement with the expectation voiced in the paragraph above, the $1/(N+1)$ size dependence holds well for polyenes with 10 and more carbons.

It is a very interesting result of our study that the energy gap for the covalent transitions vanishes in the limit $N\rightarrow\infty$ for the PPP polyene without bond alternation, i.e., this well-known feature of the Hubbard model is not altered when the range of the Coulomb repulsion is extended in the PPP model. A comparison of Fig. 9 and of the data in Table I with the results for the $U/|t|=2$ Hubbard model in Figs. 7 and 8 shows also that the slopes of the extrapolated size dependences of the covalent transitions are similar for the two models. The similarity between the ionic transitions is not as striking. The asymptotic optical gap is much larger in the PPP model than in the $U/|t|=2$ Hubbard model proving that also long-range electron interactions contribute to this gap. However, the slopes of the respective extrapolations and, in particular, the ratios of these slopes are similar such that the analysis of these ratios, that has been carried out in detail for the $U/|t|=2$ Hubbard model and has lead to the determination of transition momenta and quantum numbers, applies equally well to the nonalternating PPP model considered here.

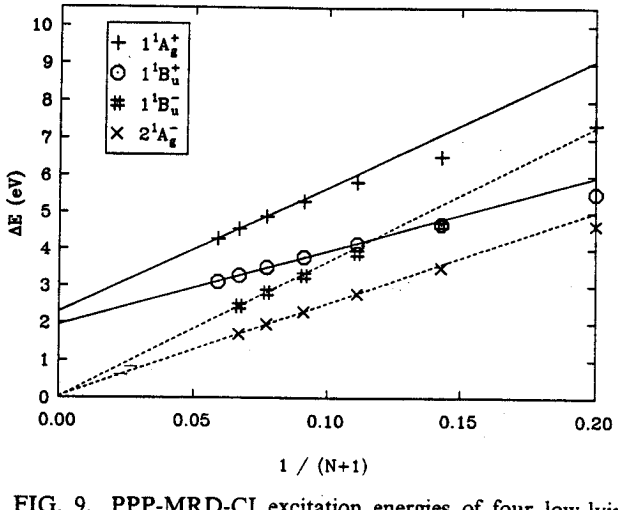

FIG. 9. PPP-MRD-CI excitation energies of four low-lying singlet states for nonalternating polyenes ($\delta=0$) on a $1/(N+1)$ scale. The linear $1/(N+1)$ extrapolations for the ionic states (solid lines) and for the covalent states (dashed lines) are fits to the results obtained for the $N=8$, 10, 12, and 14 π-electron polyenes in the case of the $2\,^1A_g^-$ and $1\,^1B_u^-$ states and, in the case of the $1\,^1B_u^-$ and $1\,^1A_g^+$ states, are the lines connecting the excitation energies at $N=12$ and 14. The ratio of the slopes of the extrapolations is 1.46 for the two covalent states and 1.68 for the two ionic states, the $1\,^1B_u^+$ state extrapolates to an optical gap $\Delta E^+=1.94$ eV.

TABLE I. Parameters of extrapolations. The parameters of the $1/(N+1)$ extrapolations [see Eq. (20)] have been obtained for the various PPP models of polyenes from fits to MRD-CI excitation energies of the primary covalent and ionic states as shown in Figs. 9, 10, and 12.

		$U(r)$		$U(2r)$	
		$\delta=0$ Å	$\delta=0.10$ Å	$\delta=0$ Å	$\delta=0.10$ Å
$2\,^1A_g^-$	ΔE_0	0.04	1.85	0.04	1.66
	α	12.45	8.63	11.15	7.21
$1\,^1B_u^+$	ΔE_0	1.94	2.87	2.14	2.94
	α	20.12	14.85	30.27	24.63

B. Spectra of alternating polyenes

We now turn to the most realistic model of polyenes and polyacetylene that is based on the PPP Hamiltonian and on a geometry with bond alternation, the latter being described by $\delta=0.10$ Å (see Sec. III). The results of the corresponding MRD-CI calculations are the most relevant in this paper. For this reason, the calculations were carried out to the largest degree of completion, i.e., they cover polyenes with 4 to 16 carbons and include three covalent ($2\,^1A_g^-$, $1\,^1B_u^-$, $3\,^1A_g^-$) and two ionic ($1\,^1B_u^+$, $1\,^1A_g^+$) states. The size dependence of the respective excitation energies is presented in Fig. 10.

The overall appearance of the spectra in Fig. 10 is similar to that of linear Hubbard chains. There are two bands of excitations, the covalent band and the ionic band. The size dependence of the excitation energies in both bands follows an $1/(N+1)$ behavior as illustrated in Fig. 10. We have exhibited the $1/(N+1)$ dependence by fitting straight lines through the data points in Fig. 10. The lines have been obtained as follows: We have first drawn the two lines through the data points for the primary, i.e., lowest, covalent state and the primary ionic state for polyenes with 12, 14, and 16 carbons. These lines correspond to a size dependence as described by the function in Eq. (20) with $q=2$ for the $2\,^1A_g^-$ state and $q=1$ for the $1\,^1B_u^+$ state. The corresponding slopes α and the asymptotic gaps ΔE_0 are presented in Table I. We have then replotted the function describing the primary covalent excitation for q values 3 and 4. The resulting lines are found in Fig. 10 to coincide asymptotically with the excitation energies of the $1\,^1B_u^-$ and of the $3\,^1A_g^-$ state, respectively. Since the analysis for the Hubbard rings and chains revealed that the $2\,^1A_g^-$ excitation carries the momentum $2k^c$, k^c defined in (10), this latter observation implies that the $1\,^1B_u^-$ excitation carries a momentum $3k^c$ and the $3\,^1A_g^-$ excitation carries a momentum $4k^c$, proving thereby our conjectures in Sec. IV. We have also replotted the function describing the primary ionic excitation—up to a very small shift of the asymptotic gap—with a q value of

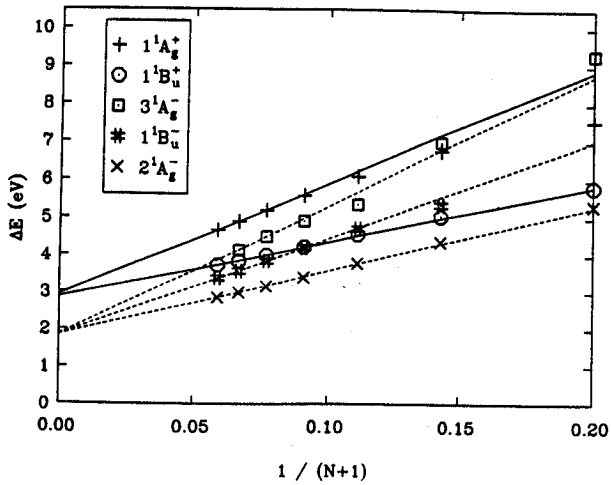

FIG. 10. PPP-MRD-CI excitation energies of five low-lying singlet states for alternating polyenes ($\delta=0.10$ Å) on a $1/(N+1)$ scale and extrapolations to polyacetylene. The linear $1/(N+1)$ extrapolations for the lowest ionic state (lower solid line) and for the lowest covalent state (lowest dashed line) are fits to the results obtained for the $N=10$, 12, 14, and 16 π-electron polyenes. The optical gap predicted by the extrapolation of the $1\,^1B_u^+$ excitation energies is $\Delta E^+=2.87$ eV and the covalent gap derived from the $2\,^1A_g^-$ extrapolation is $\Delta E^-=1.85$ eV. The extrapolations for the higher excited states have been obtained for the covalent states by multiplying the slope of the $2\,^1A_g^-$ extrapolation with a factor 1.5 for the $1\,^1B_u^-$ state and with a factor 2.0 for the $3\,^1A_g^-$ state. The extrapolation for the ionic $1\,^1A_g^+$ state has been obtained by multiplying the slope of the $1\,^1B_u^+$ extrapolation with a factor 2.0 and by adding 0.07 eV to the extrapolated optical gap.

2. The resulting line falls asymptotically on the excitation energies for the $1\,^1A_g^+$ state implying that this excitation carries a momentum two times larger than that of the $1\,^1B_u^+$ state. The value 2 determined for the ratio of the slopes of the ionic-state extrapolations shown in Fig. 10 is a little surprising in view of the analysis of the momenta associated with the ionic transitions in the Hubbard model. This analysis had revealed that these momenta increase with increasing interelectronic forces and, possibly, decrease with increasing quantum numbers q. The latter decrease had furnished a possible explanation of the rather small ratio 1.67 determined for the ionic-state extrapolations in the $U/|t|=2$ Hubbard model and in the PPP model without bond alternation. The value 2 found here in the PPP model of alternating polyenes may imply either that alternation decreases the elementary chain momentum of ionic transitions from the value $k_1^{c+}\approx 1.5k^c$ to the value $k_1^{c+}\approx k^c$, i.e., that $\gamma_1^+(U)\approx 1$ [cf. Eq. (13)], or else that there is no strong dependence of $\gamma_q^+(U)$ on q in alternating polyenes.

One of the most interesting results shown in Fig. 10 is the prediction of a finite asymptotic gap of the covalent states which measures $E^-(0)=1.85$ eV. This gap has to be attributed solely to bond alternation. With the value for α given in Table I one obtains from Eqs. (10), (12), (15), and (20) a linear approximation to the dispersion relation of the covalent excitations in the infinite alternating polyene that is given by

$$E^-(k)=E^-(0)+\tilde{\alpha}k \tag{21}$$

with $\tilde{\alpha}=\alpha/\pi=2.75$ eV. The gap of ionic excitations which corresponds to the gap of the conduction band in $(CH)_x$ is found to be increased by a third over that of the polyene without bond alternation (see Fig. 9). Since single electron theories predict a vanishing optical gap for nonalternating polyenes, this implies that, contrary to the behavior of the covalent gap, only about 30% of the optical gap in $(CH)_x$ should be due to Peierls distortion, the major fraction being due to electron correlation.[12]

C. The origin of the covalent gap and the spectrum of triplet excitations

Before we attempt to relate the results shown in Fig. 10 and Table I to observed properties of $(CH)_x$ (see Sec. V D) we would like to give a physical interpretation of the covalent gap $E^-(0)$ predicted for $(CH)_x$. For this purpose we first note that the alternation of short and long C—C distances observed for the ground state of $(CH)_x$ (Ref. 56) indicates the existence of stable π bonds. Thus, the ground state of $(CH)_x$ can be represented as a sequence of ethylene units each characterized by a singlet spin pairing of the π electrons [see Fig. 11(a)].

The $2\,^1A_g^-$ state has been characterized as involving two intraethylene triplet excitations which are coupled to an overall single state.[38,14] In fact, the excitation energy of the primary covalent excitation measures about twice the excitation energy of the lowest triplet excitation. A typical spin coupling diagram contributing to the $2\,^1A_g^-$ state is shown in Fig. 11(b). Two of the singlet pairings of the ground-state structure in Fig. 11(a) have been converted to a triplet pairing. The location of the triplet pairing

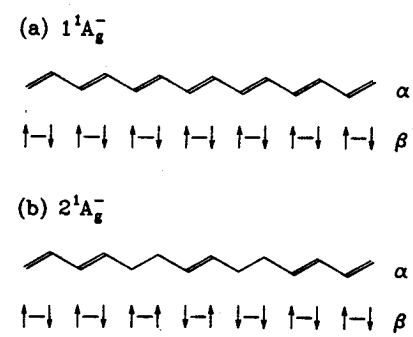

FIG. 11. Schematic representation of the electronic structure of the ground state (a) and of the first excited covalent state (b) of the polyenes. (a) The ground-state structure of alternating single and double bonds shown in α is represented by the singlet spin pairings within the ethylic units depicted in β. (b) As indicated in β the excited state is created by simultaneous spin flips in two ethylene units, the resulting triplet pair being coupled to an overall singlet. Each intraethylenic triplet corresponds to a single rather than to a double bond as sketched in α.

TABLE II. Triplet excitations in the $N=10$ polyene. Exact excitation energies (ΔE_{FCI}) of the three lowest covalent triplet states in the $N=0$ polyene calculated by Soos and Ramasesha (Ref. 12) for the PPP model with alternation are compared with estimates ($E^T_{q_T}$) evaluated from the approximate triplet dispersion relation (22) by inserting q_T quanta of the elementary chain momentum k^c.

Triplet	ΔE_{FCI}	$E^T_{q_T}(10)$	q_T
$1\,^3B_u$	1.76	1.71	1
$1\,^3A_g$	2.57	2.49	2
$2\,^3B_u$	3.39	3.28	3

is not fixed but one has to imagine that the triplet excitations are moving over the whole polyene.

We would like to demonstrate now that the above characterization of the $2\,^1A_g^-$ state as a triplet-triplet (TT) excitation can be generalized to the whole class of low-lying covalent singlet excitations. This conjecture implies that one should obtain the excitation energies of the higher covalent singlet states ($1\,^1B_u^-$, $3\,^1A_g^-$, etc.) by adding the excitation energies of those covalent triplet excitations which couple to form the respective TT state.

A polyene of N carbon atoms can accommodate as many linearly independent covalent triplet states as there are ethylene units, i.e., $N/2$. For the $N=10$ polyene the PPP excitation energies ΔE_{FCI} of the three lowest covalent triplet states ($1\,^3B_u$, $1\,^3A_g$, $2\,^3B_u$) are given in Table II. These energies have been calculated by Soos and Ramasesha using a complete valence-bond description.[12] By forming irreducible products[32] of the triplets one obtains the symmetry labels of the TT-excitations, e.g., $^1(^3B_u\otimes{}^3B_u)=\,^1A_g$, and by adding the corresponding energies one obtains an estimate ΔE_{sum} for the excitation energies of the TT states. Table III gives for the five lowest covalent singlet excitations in the $N=10$ polyene, the decomposition into triplet excitations, and compares the estimates ΔE_{sum} with exact (ΔE_{FCI}) and close to exact (ΔE_{QCI}) computational results. Again, the exact excitation energies have been taken from Ref. 12 whereas the close to exact excitation energies have been calculated by our Q-CI method.[13]

As exhibited by Table III the sums ΔE_{sum} of the triplet excitation energies furnish a close approximation to the excitation energies of the TT states indicating that our generalization is actually correct. The approximation is a little worse for the $3\,^1A_g^-$ and $4\,^1A_g^-$ states which should be (nearly) degenerate according to the estimate ΔE_{sum}. These states show a splitting of ≈ 0.4 eV centered around the ΔE_{sum} value. For a finite compound like the $N=10$ polyene considered here such splitting had to be expected because the two states have the same symmetry. The N dependence of the excitation energies shown in Ref. 13 leads to the expectation that, in fact, the $3\,^1A_g^-$ and $4\,^1A_g^-$ states are degenerate in the infinite system. The fifth covalent singlet excitation $2\,^1B_u^-$ is characterized in Table III as the irreducible product $^1(1\,^3B_u\otimes 1\,^3B_u\otimes 1\,^3B_u)$ of the lowest triplet state and, consequently, should have three times the excitation energy of this state. Hence, the $2\,^1B_u^-$ state is suggested to belong to a different class of covalent singlet excitations—the class of TTT states—which, as we will show below, should extrapolate to a covalent gap different from that of the TT states. The characterization of the $2\,^1B_u^-$ state as a TTT state as well as that of the other covalent singlets as TT states has been checked by us also for the $N=12$ polyene by means of comparisons similar to those in Tables III.[54]

The characterization of the low-lying covalent singlet excitations as TT states suggests that one should obtain the dispersion relation $E^T(k)$ of the covalent triplet states in the infinite alternating polyene from that of the TT states, given in Eq. (21), according to

$$E^T(k)=E^-(0)/2+\tilde{\alpha}k\ . \tag{22}$$

Generalizing the relationship between infinite chain dispersion relations and finite chain excitation energies expressed by Eq. (15) to triplet excitations we conjecture that the dispersion relation $E^T(k)$ provides an approximation $E^T_q(N)=E^T(q_T k^c(N))$, $q_T=1,2,\ldots,N/2$, for the excitation energies of covalent triplet states. Table II demonstrates for $N=10$ that indeed the approximate excitation energies $E^T_q(10)$ compare very closely with the exact values ΔE_{FCI} for $q_T=1,2,3$.

An intraethylene triplet excitation involves the transformation of an ethylene double bond to a single bond [cf. Fig. 11(b)]. Qualitatively one can interpret the triplet gap

TABLE III. Triplet-triplet excitations in the $N=10$ polyene. The decomposition of *covalent* singlet excitations into products of triplet excitations is illustrated. Exact (ΔE_{FCI}) (Ref. 12) and close to exact (ΔE_{QCI}) singlet excitation energies in the PPP model of alternating polyenes are compared with sums of exact excitation energies of the associated triplets (ΔE_{sum}) and with estimates obtained from the approximate dispersion relation (21) and from Eq. (24) by inserting q_S quanta of the elementary chain momentum k^c. The composition principle of singlet quantum numbers q_S from triplet quantum numbers q_T is also demonstrated.

Singlet	ΔE_{QCI}	(ΔE_{FCI})	Triplet-triplet	ΔE_{sum}	$E^-_{q_S}(10)$	$q_S=q_T+\bar{q}_T$
$2\,^1A_g^-$	3.42	(3.40)	$1\,^3B_u\otimes 1\,^3B_u$	3.51	3.42	$2=1+1$
$1\,^1B_u^-$	4.23	(4.23)	$1\,^3B_u\otimes 1\,^3A_g$	4.32	4.20	$3=1+2$
$3\,^1A_g^-$	4.93	(—)	$1\,^3A_g\otimes 1\,^3A_g$	5.13	4.98	$4=2+2$
$4\,^1A_g^-$	5.31	(—)	$1\,^3B_u\otimes 2\,^3B_u$	5.14	4.98	$4=1+3$
$2\,^1B_u^-$	5.34	(5.32)	$(\otimes 1\,^3B_u)^3$	5.27	5.13	$3=1+1+1$

$E^-(0)/2$ in Eq. (22) as the energy required to remove one of the distinct π bonds which make up the ethylene units of an infinite alternating polyene. The ground state of a nonalternating polyene is degenerate. Thus there are no energetically favored singlet spin pairings and the triplet gap vanishes.

The slope $\bar{a}$ of the dispersion relation $E^T(k)$ furnishes the group velocity v_T at which an intraethylene triplet excitation moves along the polyacetylene chain. v_T is given by $\bar{l}\bar{a}/\hbar$, where $\bar{l}=1.4$ Å is the average C—C distance, and measures 0.58×10^6 m/s. The data on the slope α of the $1/(N+1)$ extrapolations in Table I show that v_T increases with decreasing bond alternation and from the discussion of the Hubbard model in Sec. IV one finds that v_T decreases with increasing electron correlation.

In the analysis presented above the properties of the triplet states have been deduced from a decomposition of the covalent singlet excitations. Reversely, the results on the triplets can now be used to obtain new insights into the properties of the covalent singlets. The covalent gap appears then as the energy required to break the π bonds in two of the ethylene units of $(CH)_x$. Furthermore, the quantum numbers $q_S=2,3,4,\ldots$ associated with the TT excitations are explained as the sums

$$q_S=q_T+\bar{q}_T \tag{23}$$

of the quantum numbers q_T and $\bar{q}_T$ of the associated triplet excitations. Analogously the quantum numbers of the TTT excitations are given by $q_S=q_T+\bar{q}_T+\hat{q}_T$ and with Eqs. (22), (10), and (12) the N dependence is given by the law

$$E^{TTT-}_{q_S}(N)=3E^-(0)/2+\alpha q_S/(N+1)\,. \tag{24}$$

We have checked the correctness of Eq. (24) for the lowest TTT excitation $2\,^1B_u^-$ using Q-CI results for $N=6,7,\ldots,12$.[54] Table III shows for the $N=10$ polyene that, indeed, the TT state quantum numbers $q_T+\bar{q}_T$ obtained by combination are identical to the values q_S obtained from the slopes of the extrapolations in Fig. 10 and that the estimates $E^{TT-}_{q_S}$ obtained according to Eq. (20) for the TT excitations and $E^{TTT-}_{q_S}$ obtained according to Eq. (24) for the TTT state are very close to the exact energies.

The composition principle expressed by Eq. (23) predicts a general pattern of degeneracies of the TT excitations in linear chains with $q_S=2,3,4,5,6,7\ldots$, namely $1,1,2,2,3,3\ldots$, i.e., the first and second TT singlet excitation is nondegenerate, the third and fourth excitation is doubly degenerate, etc. In particular, as noted above, the two TT states with $q_S=4$, the $3\,^1A_g^-$ state, and the $4\,^1A_g^-$ state, should be degenerate in the infinite chain. In a polyene with N carbon atoms the $N/2$ covalent triplets can be combined to a total of $(N^2+2N)/8$ TT excitations. In the limit of large N the degeneracy pattern can be expressed by the equation

$$\rho(q)=\begin{cases}(\frac{1}{2})(q-\frac{1}{2}), & \text{if } 0\le q\le N/2+1\,,\\ (\frac{1}{2})[N+1-(q-\frac{1}{2})], & \text{if } N/2+1<q\le N+1\,.\end{cases} \tag{25}$$

When summed over q, $\rho(q)$ yields the correct total number of TT excitations.

At this point we would like to briefly comment on the question whether the approximate dispersion relations (21) and (22) are asymptotically correct in the limit $k\to0$. For the nonalternating polyene with vanishing gaps of covalent triplet and singlet excitations a behavior $E^-(k)\sim k$ is strongly supported not only by the corresponding behavior of the spin-wave excitations in the Hubbard model but also by the linear dispersion relations of such excitations that result in the much simpler quantum-mechanical and semiclassical Heisenberg models of the antiferromagnetic chain.[57] If bond alternation is introduced into the latter model the linear behavior of $E(k)$ remains unchanged, the group velocity of the spin waves decreases like in the PPP model, but, contrary to the latter model, no gap is found.[54] In contrast, a gap appears to exist in the quantum-mechanical Heisenberg model of the alternating antiferromagnetic chain.[58] It may well be that the development of covalent gaps in alternating polyenes entails an asymptotic $E(k)\sim k^2$ behavior for the spin-wave excitations. The fact, however, that Eq. (20) provides accurate excitation energies (see Fig. 10) indicates that such behavior should be confined to small values of k or large values of N, i.e., larger than 100.

D. Comparison to spectroscopic observations

The value of 2.87 eV for the asymptotic optical gap (cf. Table I) is about 0.7 eV larger than the value obtained from extrapolations of the $1\,^1B_u^+$ absorption bands observed for unsubstituted polyenes in solution[2,59] and about 1.1 eV larger than the value observed in solid state $(CH)_x$.[60] The former difference has to be attributed probably to our assumption of a bond alternation pattern described by a δ value which is (1) too large, (2) size independent, and (3) homogeneous,[13] whereas the latter difference has additional contributions due to "solvent effects." All three aspects of the assumed model geometry lead to an overestimate of the covalent as well as of the optical gap energy. For instance, in polyenes the bond alternation is known to decrease from a value $\delta=0.12$ Å for the very short $N=4$ and $N=6$ compounds[45,46] to a value $\delta=0.08$ Å in polyacetylene.[56] Since the covalent gap arises from bond alternation, the 20% overestimate of the bond alternation in our model geometry ($\delta=0.10$ Å) entails the prediction that the covalent gap should be smaller than 1.5 eV. Correspondingly one finds for the optical gap, which decreases less with decreasing degree of bond alternation, an upper bound of 2.7 eV if the 20% overestimate of the bond alternation is taken into account. Solvent effects, which are not accounted for in our calculations and which should lead to a stabilization of the optical state particularly in long chains, reduce the true gap further.

These gap energies predicted for the covalent and ionic bands apply to "vertical" transitions from the ground state, i.e., do not account for vibrational coupling. Because of this latter coupling the so-called "0-0" transitions from the vibrational and electronic ground state to the excited states in their respective vibrational ground state ac-

tually occur at lower energy. Knowledge of the respective energy decrement in finite polyenes[13] allows to conclude that the covalent transition in $(CH)_x$ should start at about 1.3 eV, i.e, in the solid state about 0.5 eV below the optical gap at 1.8 eV, transitions from the ground state extending to higher energies, transitions to the ground state extending to lower energies. Thus, the covalent excitations can explain the long-lived, low-temperature infrared photoluminescence observed at 1.2 eV.[39,40] Furthermore, rapid internal conversion from the optical band to the covalent band and subsequent photoexcitation back to the optical band, which has a large oscillator strength, can explain the fast transient photoinduced absorption observed recently at ≈ 0.45 eV.[61]

E. Effect of dielectric shielding

We have pointed out in our discussion above that electronic excitations in polyenes are affected by the Coulomb interaction between electrons. In realistic systems this interaction can be modified by dielectric screening. We have investigated the effect of such screening and replaced the matrix element describing the Coulomb repulsion (3) by Eq. (4) which, at large distances, corresponds to a dielectric medium with an optical density $n^2=2$. We compare the spectra of unscreened and screened polyenes in Fig. 12(a) (polyenes with bond alternation) and in Fig. 12(b) (polyenes without bond alternation). The results indicate that the asymptotic gaps of the primary covalent and ionic transitions, provided also in Table I, are only slightly affected by the screening. The most important effect might be that the screening lowers the covalent gap in alternating polyenes by about 0.2 eV. In contrast, the influence of the screening on the slopes α is rather large. Thus, particularly the group velocity of the particle-hole excitations, which is proportional to the slope, increases strongly with increasing screening whereas that of the spin waves decreases only a little.

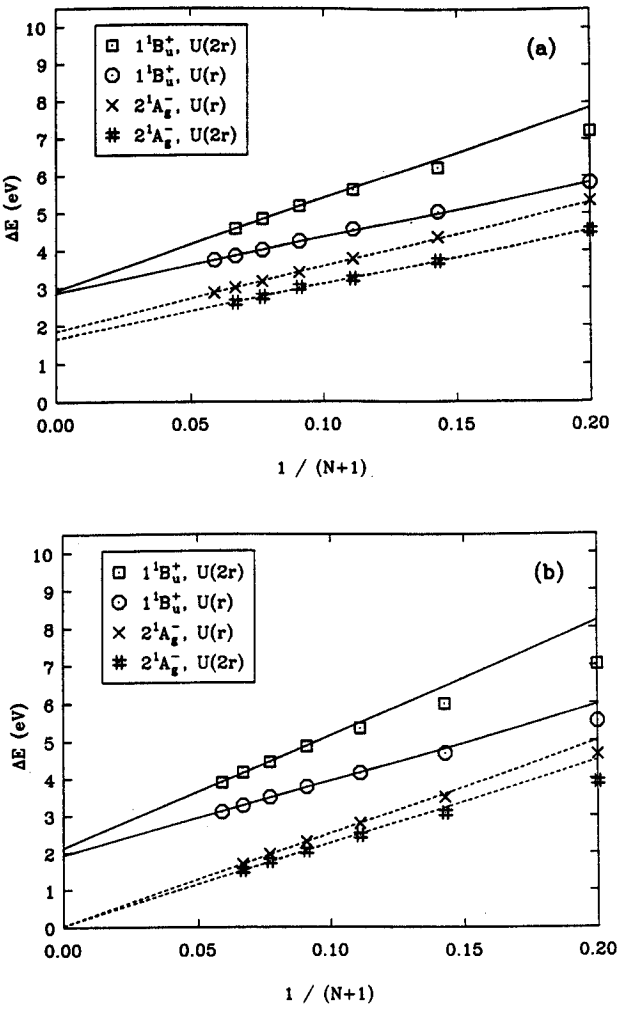

FIG. 12. The effect of dielectric shielding of the Coulomb interaction on the excitation energies of the $1\,^1B_u^+$ and $2\,^1A_g^-$ states of the polyenes for (a) $\delta=0.10$ Å and (b) $\delta=0$. The figure compares the linear $1/(N+1)$ extrapolations of the lowest covalent (dashed lines) and ionic (solid lines) singlet state excitation energies for the cases of an unshielded $U(r)$ and shielded $U(2r)$ Coulomb interaction.

VI. BOND STRUCTURE AND SOLITONIC EXCITATIONS

Trans-$(CH)_x$ is known to assume a geometry of alternating bonds.[56] At the first glance the ground state of this molecule seems to exhibit two energetically degenerate structures (A) and (B) of alternating double and single bonds, one of which (A) is presented in Fig. 13 (top). The other structure (B) is obtained upon interchanging in (A) double and single bonds. However, a degeneracy of the (A) and (B) phases should exist only in truly infinite $(CH)_x$ chains. In all finite, i.e., in all real, $(CH)_x$ molecules which are composed of an even number N of carbon atoms the ground state is represented by that structure (A) which features the maximum number $N/2$ of double bonds. The removal of one of these bonds upon replacing, for instance, the singlet spin pair in an ethylene unit by a triplet spin pair requires, as we have shown in the preceding section, an excitation energy $E^-(0)/2\approx 0.9$ eV. Hence, due to the finite size the degeneracy of structures (A) and (B) is lifted in each $(CH)_x$ molecule. Structure (B) can be created in part of a $(CH)_x$ compound from (A) only upon creating a topological soliton-antisoliton pair. A single topological soliton like the neutral soliton depicted schematically in Fig. 13 (bottom) is a domain wall separating the (A) and (B) phases. The ground state of $(CH)_x$ compounds with an odd number of carbon atoms should have the structure of a neutral soliton. Topological solitons have been inferred to explain a variety of physical properties of

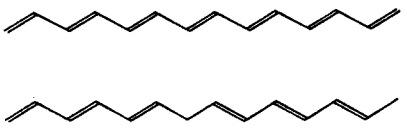

FIG. 13. One of the two degenerate bond alternation patterns of the ground state of *trans*-$(CH)_x$ (top). Schematic representation of a neutral topological soliton in *trans*-$(CH)_x$ (bottom).

$(CH)_x$, in particular its large conductivity upon doping.[3,4] In this section we want to discuss the relation of the covalent $2\,^1A_g^-$ state to soliton-antisoliton excitations.

Since in our calculations we do not explicitly consider the coupling of nuclear and electronic degrees of freedom we have to resort to empirical relations between π-bond orders and bond lengths like that given by Eq. (6) in order to retrieve information about the polyene geometry in the various polyene states. The resulting values for the order parameter Δl_n [cf. Eq. (7)] are shown in Figs. 14(a)–14(c) for the $1\,^1A_g^-$, $2\,^1B_u^+$, and $2\,^1A_g^-$ states of the polyenes with $N=8,10,\ldots,16$ carbons. Solid and dashed lines refer to the results of MRD-CI calculations for alternating ($\delta=0.10$ Å) and nonalternating ($\delta=0$) PPP polyene models, respectively.

Figure 14(a) demonstrates that the order parameter Δl_n for the ground state assumes uniform positive values corresponding to that geometry of alternating double and single bonds which exhibits a maximum number of double bonds. The predicted alternation of the bond length decreases slightly towards the center of the polyenes, an effect which is more pronounced for longer compounds. For the polyene with $N=14$ carbons the average alternation of the bond lengths defined as $\bar{\delta}$ ($\bar{\delta}=2\,\overline{\Delta l_n}$) is determined to be 0.104 Å. If we assume in our calculation of the electronic ground state no bond alternation the bond orders still show a pronounced alternation of double bonds and single bonds. Applications of (6) to determine the corresponding bond lengths yields the value $\bar{\delta}=0.066$ Å. The small difference between the two $\bar{\delta}$ values demonstrates that the predictions obtained from the empirical bond-order–bond-length relation (6) depend only weakly on the geometry assumed in calculating the electronic ground state. Furthermore, both $\bar{\delta}$ values are close to the degree of bond alternation $\delta=0.08$ Å observed in long polyenes.[56] Hence, the bond alternation of the ground state of polyenes is mainly due to the forces exerted by the correlated electron system on the lattice whereas the reverse influence of the lattice on the electrons is smaller. The latter coupling increases the degree of bond alternation by about 40% as measured by the parameter $\bar{\delta}$. This result is in harmony with the recent proof that the bond alternation in $(CH)_x$ is mainly due to electron correlation and that the contribution to the alternation caused by the pure (single) electron-phonon coupling, the so-called "Peierls distortion," is of minor importance.[28]

In the excited $1\,^1B_u^+$ state the order parameter Δl_n remains positive but, compared to the ground state, decreases towards the central region of the polyenes, corresponding to a weakening of the bond alternation. This behavior is illustrated in Fig. 14(b). For the polyene with $N=14$ carbons the average bond alternation obtained is $\bar{\delta}=0.028$ Å. The difference between this value and the ground state value $\delta=0.08$ Å explains the large intensity of the C—C single and double bond stretching modes observed in resonance Raman experiments.

The bonding pattern in the excited $2\,^1A_g^-$ state differs from that in the $1\,^1A_g^-$ and the $1\,^1B_u^+$ states. As shown in Fig. 14(c) the order parameter Δl_n in the $2\,^1A_g^-$ state becomes negative in the central region of the polyenes. Negative values of Δl_n indicate a reversal of the bond alternation pattern. A change of the sign of Δl_n corresponds to a soliton structure like that depicted in Fig. 13 (bottom). The order parameter of the $2\,^1A_g^-$ state of $N=10,\ldots,16$ polyenes shown in Fig. 14(c) character-

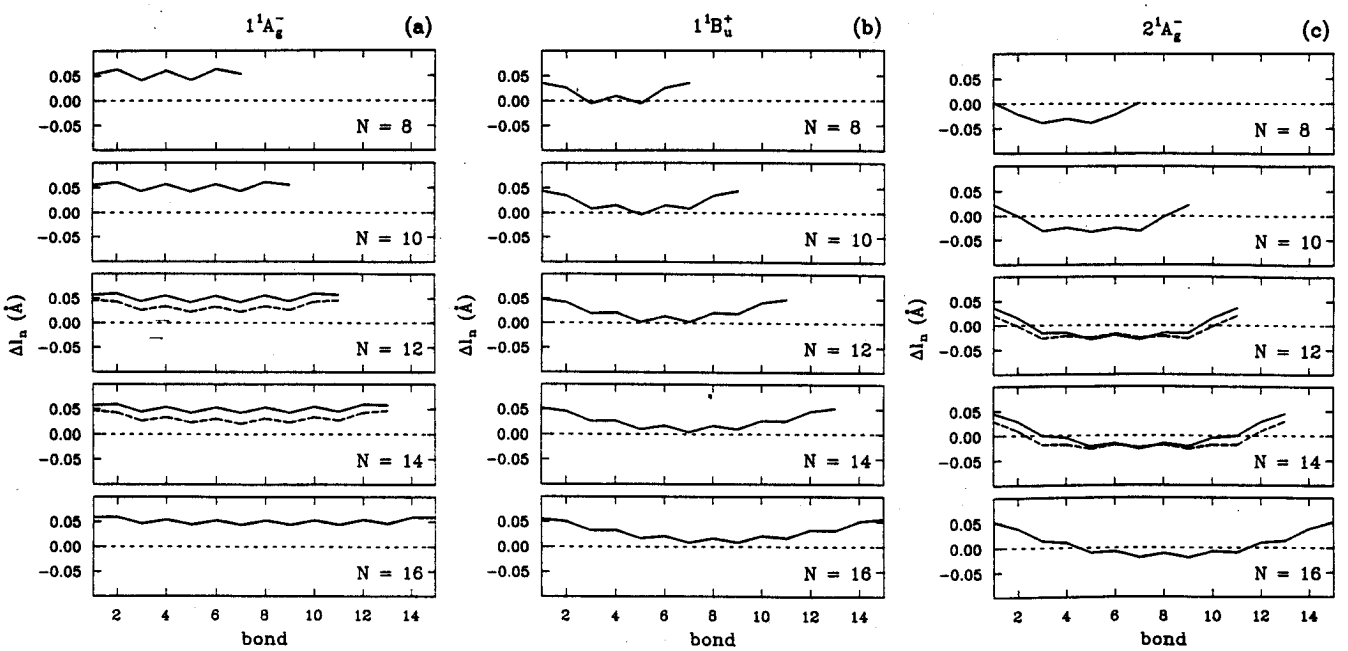

FIG. 14. (a) Order parameter Δl_n of the ground state of the polyenes containing $N=8,10,\ldots,16$ π electrons evaluated according to Eq. (7) from PPP-MRD-CI bond orders. The solid lines refer to alternating ($\delta=0.1$ Å) and the dashed lines to nonalternating model geometries; (b) order parameter Δl_n of the lowest ionic excited singlet of the $N=8,10,\ldots,16$ polyenes; (c) order parameter Δl_n of the lowest covalent excited singlet state of the $N=8,10,\ldots,16$ polyenes.

izes this state as a soliton-antisoliton pair state (see "note added"). The distance between the two solitons measures eight C—C bond units. In case that we assume in our calculation a nonalternating polyene geometry, the soliton-antisoliton structure remains, however, the distance between soliton and antisoliton becomes size-dependent measuring 9 C—C bond units for $N=12$ and 10 C—C bond units for $N=14$. Since in the process of the electronic excitation of the $2\,^1A_g^-$ state the $(CH)_x$ geometry relaxes from an initially alternating structure to a structure with a smaller and partially inverted bond alternation, the increasing distance of the two solitons calculated for the nonalternating polyene appears to indicate that a soliton-antisoliton pair in a long polyene may be formed initially at a small distance and may then oscillate or perhaps separate.

The bond structures of the ground state $1\,^1A_g^-$ and the primary covalent excited state $2\,^1A_g^-$ can be explained in a simple and illuminating manner. This explanation proceeds along the same lines of reasoning as that on the covalent gap in connection with Fig. 11 and is based on the fact that a double bond in a polyene corresponds to a pair of π electrons at adjacent carbon atoms the spins of which are coupled to a singlet state. The ground state $1\,^1A_g^-$ realizes a maximum number of such spin pairings which define the ethylene units of $(CH)_x$, whereas the $2\,^1A_g^-$ state is characterized as involving two intraethylene triplet excitations which are coupled to an overall singlet state. The corresponding spin pairings and their relationship to bond structure are illustrated in Fig. 15. In order to arrive at a bond pattern for the $2\,^1A_g^-$ state one has to keep in mind that the intraethylene triplets in Fig. 15(b) are coupled to an overall singlet state. This implies that the spins can recouple into a new set of singlet pairings as indicated in Fig. 15(b) by the corresponding connections of pairs of spins. The pairing of spins shown corresponds to the neutral soliton-antisoliton structure also presented in Fig. 15(b). Hence, the singlet spin pairing together with the fact that the primary covalent excitation involves a triplet-triplet excitation with an overall singlet coupling yields the soliton-antisoliton structure of this excitation. The question arises if this composite character of the covalent excitation, i.e., that of a triplet-triplet excitation or that of a soliton-antisoliton excitation, can manifest itself in polyacetylene through an observation of its separate components: Does a covalent singlet excitation yield separate triplet excitations? Does the covalent excitation yield separate solitons?

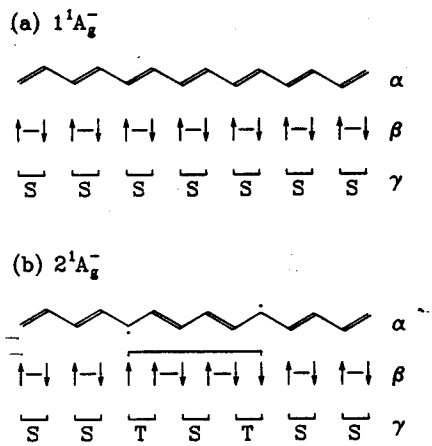

FIG. 15. Schematic representation of the electronic structure of the ground state (a) and of the first excited covalent state (b) of the polyenes. The representative ordering of neighboring spins depicted in β can either be interpreted in terms of the valence-bond structures, that are indicated by the bars in β, and correspond to the geometries shown in α, or can be interpreted in terms of singlet S or triplet T spin pairings within the ethylene units as depicted in γ. The excited $2\,^1A_g^-$ state is generated from the ground state by a simultaneous flip of two spins and, accordingly, can be interpreted either as a neutral soliton-antisoliton pair $b\alpha$ or a simultaneous triplet-triplet excitation coupled to an overall singlet state (see text for discussion).

VII. DISSOCIATION OF COVALENT EXCITATIONS INTO TRIPLETS AND SOLITONS

We have shown in the preceding section that the covalent excitations in polyenes can be regarded either as soliton-antisoliton ($S\bar{S}$) or as triplet-triplet (TT) excitations. The wave functions which result from our MRD-CI calculations on finite polyenes describe delocalized excitations, i.e., excitations spread over the entire polyene chain. One expects, however, that for very long polyenes wave packets of these delocalized states can form which are localized in parts of a polyene. The origin of such localization can be either specific interactions exerted when the excitation is initially prepared or can be the coupling to lattice distortions. In the following we want to investigate the latter possibility. If such localization can be achieved it might also be possible to observe the single components of covalent excitations, namely either solitonic excitations or triplet excitations. An argument in favor of this possibility is that the binding energy between two triplets in a TT-excitation is small as shown by the fact that the excitation energy of a TT state is approximately the sum of the excitation energies of two separate triplet states.

The prerequisite that electron-lattice interactions of a magnitude δE can mix pure electronic states $|j\rangle$ to form wavepackets like

$$|\omega\rangle=\sum_j a_j|j\rangle \tag{26}$$

is that the energy separation between the states $|j\rangle$ does not exceed δE by a large margin. Furthermore, our results on the spectra of polyenes as shown in Fig. 10 allow an estimate of the level density of covalent states. As we have demonstrated in Sec. V the low-lying covalent states in alternating polyenes with $\delta=0.10$ Å approximately obey the simple behavior

$$E_q^-(N)=\Delta E_0+q\frac{\alpha}{N+1},\quad q=2,3,4,\ldots, \tag{27}$$

where the numerical constants, given in Table I, are determined by the parametrization of the PPP Hamiltonian (2). In the limit of large N the degeneracy $\rho(q)$ of these states

is given by Eq. (25) such that we can estimate the density of covalent states in long polyenes in the energy range above ΔE_0.

With respect to their coupling to the lattice there should be a qualitative difference between dissociated $S\bar{S}$ and TT excitations in long polyenes. Dissociated $S\bar{S}$ excitations are topological excitations that require the distortion of the complete lattice between soliton and antisoliton whereas dissociated TT excitations require strictly local distortions only. This difference is schematically indicated by the difference between the bond structures (α) in Figs. 15(b) for the $S\bar{S}$-pairs and 11(b) for the TT excitations. An upper bound for the electron-lattice interaction energy δE, estimated from Eq. (5) as the difference of the resonance integral t for single and for double bonds, is 0.34 eV. This upper bound for δE should apply to the case of a topological lattice distortion connected with a distant $S\bar{S}$ pair. However, in the case of a strictly local lattice distortion delocalized states will only experience an effective interaction of about 0.34 eV/N since local amplitudes of delocalized states are proportional to $N^{-1/2}$. The question arises if an interaction of that order of magnitude suffices to induce localized covalent excitations in long polyenes, i.e., two localized triplets and close $S\bar{S}$ pairs. Since the spacing between covalent states according to Eq. (27) is also proportional to $1/N$, perturbation theory does not provide an answer. Instead we need to derive a nonperturbative estimate. For this purpose we introduce the following strong assumption regarding the matrix elements of the perturbation δV originating from a local distortion of the lattice

$$\langle j \mid \delta V \mid k \rangle = \delta E < 0 \,, \tag{28}$$

i.e., the values of these matrix elements are assumed to be independent of $|j\rangle$ and $|k\rangle$ and negative. Here $|j\rangle$ and $|k\rangle$ are delocalized covalent excitations as defined in (26). The latter assumption is plausible for both $S\bar{S}$ and TT pairs because from the π-bond orders of the covalent states $|j\rangle$ one expects δE to be negative if the distorted lattice exhibits a less distinct bond alternation than that defined by $\delta = 0.10$ Å. Such lattice distortion, however, should accompany localized triplets as well as solitonic excitations. The eigenvalue problem of the perturbed band of covalent excitations is defined by the equation

$$E_j a_j + \delta E \sum_k a_k = \varepsilon a_j \,, \tag{29}$$

where E_j and a_j are the energies and expansion coefficients of the unperturbed states $|j\rangle$. In the following all energies will be defined relative to the band edge ΔE_0. The expansion coefficients can be expressed formally as follows

$$a_j = \frac{\delta E}{\varepsilon - E_j} \sum_k a_k \,. \tag{30}$$

Iterating this equation once yields[62]

$$1 = \delta E \sum_j \frac{1}{\varepsilon - E_j} \,. \tag{31}$$

The solution of Eq. (31) provides the energy spectrum ε_j of the perturbed band of covalent states. This spectrum is located close to the unperturbed band of energies E_j except for the eigenvalue of one state which is moved far below the unperturbed band. To demonstrate the existence of this state we consider Eq. (31) in the limit of large N. Then one can replace the sum by an integral to obtain

$$1 = \delta E \int_0^{N+1} \frac{\rho(q)dq}{\varepsilon - E_q^-} \,, \tag{32}$$

where the energies E_q^- of the covalent states are given by Eq. (27) and their degeneracies $\rho(q)$ by Eq. (25). The integral can be evaluated and in the limit $|\varepsilon| \gg \alpha$ one finds

$$\varepsilon \approx \frac{\delta E}{4} N^2 \approx -(0.09 \text{ eV})\, N \,. \tag{33}$$

In fact, this expression proves that the interactions in the band of covalent excitations induce a state which for large N is strongly shifted and, hence, localized.

The important property of relationship (33) is that the energy shift increases linearly with N, i.e., one expects that for some length N of a polyene localization will set in. However, it is impossible to estimate this length since expression (33) overestimates the energy shift. There are three reasons. First, the assumption $|\varepsilon| \gg \alpha$ used in the derivation entails a crude approximation of the energy ε of the localized state. Second $\delta E \approx -0.34$ eV/N only provides an upper bound for the coupling to lattice distortions since we assumed an extreme reversal of single and double bonds in estimating its value. Third, the matrix elements of the perturbation are not as homogeneous as assumed by Eq. (28) but rather one has to expect a spread of the values of these matrix elements and even sign reversals. All that implies a reduction of the energy shift. Nevertheless, Eq. (33) indicates that if the interaction $\langle j \mid \delta V \mid k \rangle$ is homogeneous over a sufficiently broad band of energies a local lattice distortion can produce localized excitations. The possibility that topological distortions like solitons can be formed by coupling to the lattice follows in a straight forward way by perturbation theory.

We want to argue now that there exists indeed strong experimental evidence for a separation of the covalent states in polydiacetylene into separate, i.e., localized triplets. Such triplets would be observable after photoexcitation of the material into the band of ionic states, internal conversion to the band of covalent states and dissociation of a TT state into separate triplets. Evidence for the appearance of fast photoinduced triplets has been provided recently by Robins *et al.* on the basis of magnetic field modulated optical absorption and microwave absorption experiments.[63] However, the observations of these authors do not reveal the route of triplet production. In a recent microwave absorption experiment with nanosecond time resolution Sixl *et al.* found that initially all triplets sublevels are equally populated, i.e., the triplets formed are completely unpolarized.[64] Triplets formed through the strongly orientation-dependent interactions of an intersystem crossing route are always polarized to some degree. The puzzling observation of Sixl *et al.* can be explained readily, however, if the triplets are born from a covalent TT excitation. In this excitation the two triplets denoted

by ${}^3T_n^{(1)}$ and ${}^3T_m^{(2)}$ are coupled to an overall singlet state ${}^1S_0^*$ according to the scheme

$$ {}^1S_0^* = \frac{1}{\sqrt{3}}({}^3T_1^{(1)}\,{}^3T_{-1}^{(2)} - {}^3T_0^{(1)}\,{}^3T_0^{(2)} + {}^3T_{-1}^{(1)}\,{}^3T_1^{(2)}) . \tag{34} $$

Since the numerical (Clebsch-Gordon) coefficients for all triplet sublevels, except for a phase factor, are identical in this scheme neither of the triplets is polarized. This follows formally from the fact that the matrix elements for the spin operator $\vec{S}_1$ of triplet ${}^3T_m^{(1)}$, i.e., $\langle {}^1S_0^* \mid S_{1\beta} \mid {}^1S_0^* \rangle$, $\beta = x,y,z$, vanish. Consequently, the observation of Sixl *et al.* proves unequivocally that the covalent singlet excitations are the parent states of the photoinduced triplets observed in polydiacetylene. We note that the proposed *TT* state dissociation is analogous to the singlet exciton fission observed in organic crystals.[65,66]

The covalent excitations may also decay into separate spin-$\frac{1}{2}$ solitons which have been characterized schematically in Fig. 13 (bottom), though no proof exists so far for this process. The solitons formed by this route should give rise to photoinduced ESR signals which also should be unpolarized because of their singlet parent state. The decay route, i.e., either to triplets or to solitons, should depend on the material involved. For example, polydiacetylene's bond structure is unfavorable for soliton formation, hence the triplet route is more favorable. Polyacetylene can accommodate solitons, hence the decay to solitons should be observed in case the decay to triplets is less efficient. This might actually be the case since the perturbation for triplet localization is $\delta E \sim 1/N$, whereas that for solitons is likely to be independent of N.

The fact that photoinduced triplet pairs and possibly also soliton pairs are born in a pure singlet quantum state can be proven by a magnetic field dependence of their recombination dynamics. If a large enough fraction of triplet pairs or solitonic spin-$\frac{1}{2}$ pairs in polyacetylene at a time t after their birth can reform to the singlet covalent state or to the singlet ground state this process acts as a filter for the singlet character of the pair at time t. An external magnetic field acting together with either the fine structure interaction (triplet) or the hyperfine interaction (spin-$\frac{1}{2}$ solitons) leads to a yield of free triplets or solitons with a characteristic magnetic field dependence. The theory of this process has been described for such recombination processes in liquids in Ref. 67.

VIII. SUMMARY AND OUTLOOK

The properties of polyacetylene and of related one-dimensional conducting and semiconducting polymers are dominated by the effects of electron correlation. The polymers are not of "infinite" length but typically consist of a few hundred to a few thousand elementary units. The description of the excitations of a correlated electron system that is neither "infinite" nor "small" falls into a domain of physics that is located between molecular physical and solid state physics. In this paper we have demonstrated, using polyacetylene as an example, how these branches of physics can be bridged. Our approach is based on four fundamental assumptions the validity of which has been investigated in detail.

(1) The physical nature of excitations in infinite and in large, but finite, many-electron systems is identical. Thus, the energy-momentum relations valid in the infinite system for the various classes of excitations, like covalent (spin-wave) or ionic (particle-hole) excitations, should apply also to finite systems.

(2) In finite systems the wavelength of an excitation cannot exceed the system length L if the system is cyclic and $2L$ if it is linear. According to the de Broglie relation, therefore, the energetically lowest excitations of each class is associated with an elementary transition momentum. Equations (9) and (10) give the lower bounds for the elementary transition momenta in cyclic ($N = 4n+2$) and linear N-electron systems, respectively.

(3) The values of the elementary transition momenta are solely determined by the geometry of the finite system, i.e., are given by the lower bounds.

(4) The momenta associated with transitions to higher excited states are integer multiples of the elementary transition momenta [cf. Eqs. (11) and (12)]. Consequently, as expressed by Eqs. (14) and (15), the discrete energies of a finite system are obtained by evaluating the energy-momentum relations of the infinite system at multiples of the elementary transition momenta. Conversely, the dispersion relations of the infinite system can be determined from the energy spectra of finite systems if the values of the transition momenta are known.

For the investigation of the validity of these assumptions we have first selected the Hubbard model since it is the most simple model of one-dimensional many-electron systems that describes both the kinetic energy and the Coulomb interaction of the electrons, and since it is the only model for which exact results on finite as well as on infinite systems are available. In those cases, in which exact excitation energies for finite systems were unavailable, we have employed a multireference double-excitation configuration interaction expansion (MRD-CI) which recently has been developed by us[13] for the calculation of accurate excitation energies. We have demonstrated that assumptions (1), (2), and (4) render excellent and asymptotically (for large N) correct approximations. Assumption (3) has been shown to be valid for covalent (spin-wave) excitations in rings and chains and for ionic (particle-hole) excitations in rings, whereas it turned out to be invalid for ionic excitations in chains. The transition momentum associated with the lowest ionic excitation in chains was found to increase with increasing Coulomb interaction of the electrons [see Eq. (13)]. Such increase, though possibly smaller, appeared to exist also for higher ionic excitations. A more detailed study of these effects requires analytical results on the Hubbard model of finite linear chains. It would be desirable, in this respect, to derive equations for finite Hubbard chains that are analogous to the Lieb-Wu equations[33] for finite rings.

For Hubbard interaction parameters, which apply to π electrons in polyenes, the dispersion relations of ionic and covalent excitations are nearly linear over a wide range of momenta. In this linear regime assumptions (1)–(4) allow

the construction of approximate dispersion relations from the energy spectra of finite polyenes by means of $1/(N+1)$ extrapolations. Assuming that a linear approximation of the energy-momentum relation also holds for polyenes described by the Pariser-Parr-Pople (PPP) model we have evaluated dispersion relations for nonalternating and alternating polyenes using the results of MRD-CI calculations.

The gap of the band of covalent singlet excitations is found to vanish for nonalternating polyenes and to be large for alternating polyenes. We have estimated for this gap in $(CH)_x$ a value of about 1.3 eV.

The covalent singlet states of long polyenes can be characterized as being composed of two or more triplet spin waves combined to an overall singlet state. This characterization allowed the derivation of the momentum quantum numbers of the covalent singlet states from those of the triplet states and of the state density in the covalent band. The same connection between covalent triplet and singlet states has been exploited by Woynarovich for the Hubbard model in his derivation of singlet spin-wave dispersion relations from those of triplet states.[37]

The dispersion relations of the covalent states in nonalternating polyenes are strictly linear in the limit of small momenta. It is uncertain if that is also the case for alternating polyenes which exhibits a covalent gap. The compounds investigated by us are not long enough to allow definite statements. For an answer to this question one should try to obtain an analytical solution of the Hubbard model of alternating polyenes (using periodic boundary conditions).

For the ionic excitations only the asymptotic "optical" gap has been estimated from extrapolations. No dispersion relations could be derived because in linear chains the transition momenta depend on the Coulomb interaction of the π electrons and can be determined from extrapolations only up to a scaling factor. Due to electron correlation the optical gap is large (≈ 2.2 eV) in nonalternating polyenes and is found to increase by about 40% upon bond alternation.

The bond orders calculated from the MRD-CI wave functions have provided insight into the bond structure of long polyenes in ground and excited states. It has been found that covalent singlet states exhibit the bond structure of a soliton-antisoliton pair. The density of states in the covalent band has been estimated to be high enough to allow in long polyenes a localization of such excitations through coupling to the lattice degrees of freedom. We have interpreted the results of recent microwave experiments[64] as evidence for the decay of covalent singlet states into separate localized triplets.

Note added. Recently Hayden and Mele have presented results of renormalization-group (RG) calculations on a 16-site Hubbard-Peierls chain.[68] The order parameters calculated for the ground and $1\,^1B_u^+$ states are similar to those shown in Fig. 14(a) and 14(b). But for the $2\,^1A_g^-$ states a structure of four solitons is predicted instead of the soliton-antisoliton structure exhibited in Fig. 14(c). The prediction of an additional soliton-antisoliton pair, located at the center of the 16-site chain, may be an artifact of the RG procedure that constructs 16-site wave functions from two 8-site chains employing quite restricted many-electron basis sets.

---

*Also at Institute for Theoretical Physics, University of California, Santa Barbara, CA 93106.

[1]For a collection of recent research reports see *Proceedings of the International Conference on Synthetic Metals, 1984* [Mol. Cryst. Liq. Cryst. **117-121** (1985)] and 1986 [Synth. Met. **16**, (1986)].

[2]For a review see B. Hudson, B. E. Kohler, and K. Schulten, in *Excited States*, edited by E. C. Lim (Academic, New York, 1982), Vol. 6, p. 1.

[3]W. P. Su, J. R. Schrieffer, and A. J. Heeger, Phys. Rev. Lett. **42**, 1698 (1979).

[4]W. P. Su, J. R. Schrieffer, and A. J. Heeger, Phys. Rev. B **22**, 2099 (1980); **28**, 1138(E) (1983).

[5]S. Kivelson and D. E. Heim, Phys. Rev. B **26**, 4278 (1982).

[6]H. Fukutome and M. Sasai, Prog. Theor. Phys. **67**, 41 (1982).

[7]H. Fukutome and M. Sasai, Prog. Theor. Phys. **69**, 1 (1983).

[8]H. Fukutome and M. Sasai, Prog. Theor. Phys. **69**, 373 (1983).

[9]M. Grabowski, D. Hone, and J. R. Schrieffer, Phys. Rev. B **31**, 7850 (1985).

[10]A. D. Kulkarni, S. A. Alexander, and F. A. Matsen, Int. J. Quantum Chem. **28**, 451 (1985).

[11]D. K. Campbell, T. A. DeGrand, and S. Mazumdar, Mol. Cryst. Liq. Cryst. **118**, 41 (1985).

[12]Z. G. Soos and S. Ramasesha, Phys. Rev. B **29**, 5410 (1984).

[13]P. Tavan and K. Schulten, J. Chem. Phys. **85**, 6602 (1986).

[14]K. Schulten, I. Ohmine, and M. Karplus, J. Chem. Phys. **64**, 4422 (1976).

[15]P. Tavan and K. Schulten, J. Chem. Phys. **70**, 5407 (1979).

[16]B. E. Kohler, P. Mitra, and P. West, J. Chem. Phys. **85**, 4436 (1986).

[17]H. Thomann, L. R. Dalton, Y. Tomkiewicz, N. Shiren, and T. C. Clarke, Phys. Rev. Lett. **50**, 533 (1983).

[18]B. R. Weinberger, C. Roxlo, S. Etemad, G. L. Baker, and J. Orenstein, Phys. Rev. Lett. **53**, 86 (1984).

[19]J. Orenstein, Z. Vardeny, G. L. Baker, G. Eagle, and S. Etemad, Phys. Rev. B **30**, 786 (1984).

[20]D. K. Campbell, T. A. DeGrand, and S. Mazumdar, Phys. Rev. Lett. **52**, 1717 (1984).

[21]R. A. Harris and L. M. Falicov, J. Chem. Phys. **51**, 5034 (1969).

[22]K. R. Subbaswami and M. Grabowski, Phys. Rev. B **24**, 2168 (1981).

[23]P. Horsch, Phys. Rev. B **24**, 7351 (1981).

[24]J. E. Hirsch, Phys. Rev. Lett. **51**, 296 (1983).

[25]M. Takahashi and J. Paldus, Int. J. Quantum Chem. **28**, 459 (1985).

[26]S. N. Dixit and S. Mazumdar, Phys. Rev. B **29**, 1824 (1984).

[27]D. Baeriswyl and K. Maki, Phys. Rev. B **31**, 6633 (1985).

[28]S. Mazumdar and D. K. Campbell, Phys. Rev. Lett. **55**, 2067 (1985).

[29]A. A. Ovchinnikov, I. I. Ukrainskii, and G. V. Kventsel, Usp. Fiz. Nauk. **108**, 81 (1972) [Sov. Phys. Usp. **15**, 575 (1973)].

[30]D. R. Yarkony and R. Silbey, Chem. Phys. **20**, 183 (1977).
[31]S. Suhai, Phys. Rev. B **27**, 3506 (1983).
[32]P. Tavan and K. Schulten, J. Chem. Phys. **72**, 3547 (1980).
[33]E. H. Lieb and F. Y. Wu, Phys. Rev. Lett. **20**, 1445 (1968).
[34]A. A. Ovchinnikov, Zh. Eksp. Teor. **57**, 2137 (1969) [Sov. Phys. JETP **30**, 1160 (1970)].
[35]F. Woynarovich, J. Phys. C **15**, 85 (1982).
[36]F. Woynarovich, J. Phys. C **15**, 97 (1982).
[37]F. Woynarovich, J. Phys. C **16**, 5293 (1983).
[38]K. Schulten and M. Karplus, Chem. Phys. Lett. **14**, 305 (1972).
[39]E. A. Imhoff and D. B. Fitchen, Solid State Commun. **44**, 329 (1982).
[40]D. B. Fitchen, Synth. Met. **9**, 341 (1984).
[41]L. Salem, *The Molecular Orbital Theory of Conjugated Systems* (Benjamin, New York, 1966).
[42]K. Ohno, Theor. Chim. Acta **2**, 219 (1964).
[43]Z. G. Soos and I. R. Ducasse, J. Chem. Phys. **78**, 4092 (1983).
[44]S. Ramasesha and Z. G. Soos, J. Chem. Phys. **80**, 3278 (1984).
[45]W. Haugen and M. Traetteberg, Acta Chem. Scand. **20**, 1726 (1966).
[46]M. Traetteberg, Acta Chem. Scand. **22**, 2294 (1968).
[47]R. J. Buenker and S. D. Peyerimhoff, Theor. Chim. Acta **35**, 33 (1974).
[48]P. Tavan (unpublished).
[49]R. Pariser, J. Chem. Phys. **24**, 250 (1956).
[50]J. Čížek, J. Paldus, and I. Hubač, Int. J. Quantum Chem. **8**, 250 (1974).
[51]F. A. Cotton, *Chemical Applications of Group Theory* (Wiley, New York, 1963).
[52]H. Bethe, Z. Phys. **71**, 205 (1931).
[53]K. Hashimoto, Int. J. Quantum. Chem. **28**, 581 (1985).
[54]P. Tavan and K. Schulten (unpublished).
[55]A. Szabo, J. Langlet, and J. D. Malrieu, Chem. Phys. **13**, 173 (1976).
[56]C. S. Yannoni and T. C. Clarke, Phys. Rev. Lett. **51**, 1191 (1983).
[57]F. Keffer, H. Kaplan, and Y. Yafet, Am. J. Phys. **21**, 250 (1953).
[58]W. Duffy and K. P. Barr, Phys. Rev. B **165**, 647 (1968).
[59]B. Hudson and B. E. Kohler, Synth. Met. **9**, 241 (1984).
[60]E. G. Mele, Synth. Met. **9**, 207 (1984).
[61]L. Rothberg, T. M. Jedju, S. Etemad, and G. L. Baker (unpublished).
[62]B. Derrida (private communication).
[63]L. Robins, J. Orenstein, and R. Superfine, Phys. Rev. Lett. **56**, 1850 (1986).
[64]H. Sixl, M. Winter, A. Grupp, and M. Mehring (unpublished).
[65]N. Geacintov, M. Pope, and F. Vogel, Phys. Rev. Lett. **22**, 593 (1969).
[66]R. P. Groff, P. Avakian, and R. E. Merrifield, Phys. Rev. B **1**, 815 (1970)
[67]K. Schulten, J. Chem. Phys. **80**, 3668 (1984).
[68]G. W. Hayden and E. J. Mele, Phys. Rev. B **34**, 5484 (1986).